A Hydride-abstraction Catalysis of *o*-Hydroxytriarylmethane via Zwitterionic Reactive Species

KATO Kohsuke

A Hydride-abstraction Catalysis of *o*-Hydroxytriarylmethane via Zwitterionic Reactive Species

双性イオンを鍵活性種とする *o*-ヒドロキシトリアリールメタンのヒドリド引き抜き触媒機能の創出

KATO Kohsuke
加藤康介

Department of Molecular & Macromolecular Chemistry, Graduate School of Engineering, Nagoya University

Contents

Chapter 1

General Introduction and Summary

1.1.1 Asymmetric Intermolecular Ion Pair Catalysis

Among the molecular transformations catalyzed by organic molecules, the catalytic chemistry of chiral quaternary onium salts has attracted attention as one of the powerful methods to achieve highly efficient and stereoselective molecular transformations by directly controlling reactive anion species. In 1984, Merck researchers first reported that quaternary ammonium salts derived from cinchona alkaloids could act as excellent stereoselective phase-transfer catalyst (Scheme 1).[1]

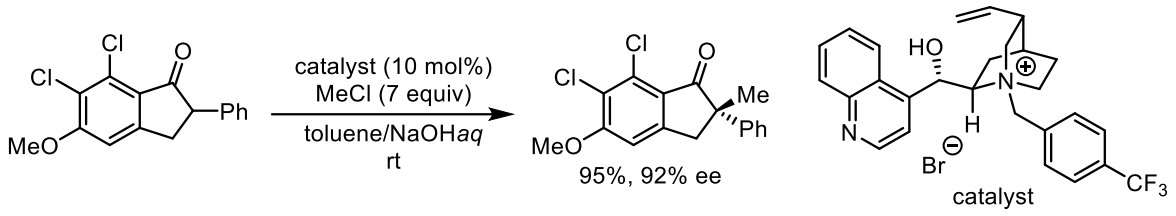

Scheme 1 Asymmetric phase-transfer catalysis reported by Merck researchers

Since then, the chemistry of phase-transfer catalysis has attracted a great deal of attention and has been established as a new field in organic synthetic chemistry. For example, Corey, Lygo, and Maruoka developed highly enantioselective alkylation of α-amino acid-derived Schiff bases using a cinchona alkaloid-derived or independently developed quaternary ammonium salt as a chiral phase-transfer catalyst under solid-liquid or liquid-liquid two-phase conditions (Scheme 2-4).[2-5]

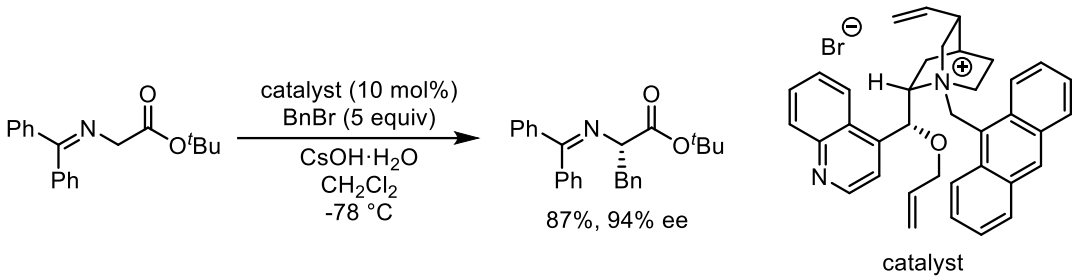

Scheme 2 Asymmetric phase-transfer catalysis reported by Corey

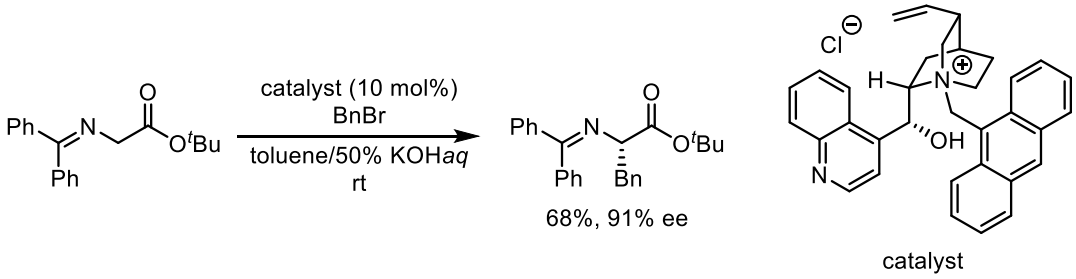

Scheme 3 Asymmetric phase-transfer catalysis reported by Lygo

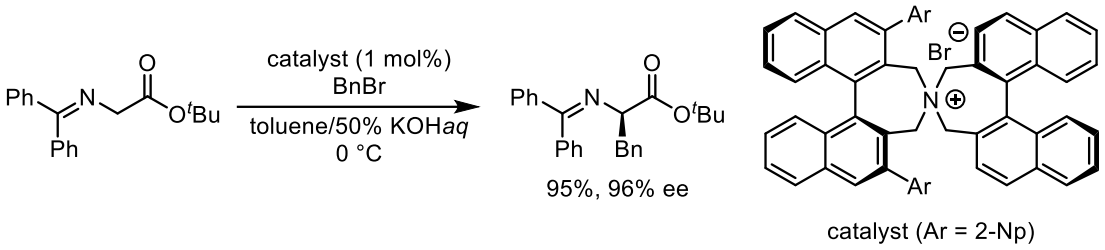

Scheme 4 Asymmetric phase-transfer catalysis reported by Maruoka

These reports are important as they demonstrate the stereoconctrol ability of chiral onium salts. However, in general, the distance and direction between ions under reaction conditions are difficult to define in such onium salt catalytic systems because anions and cations are linked by electrostatic inter-ionic forces, and the overall three-dimensional shape of the ion pairs is ambiguous, making it difficult to optimize the catalyst structure according to the reaction. In addition, in intermolecular ion pairing catalysts, the anions that the catalyst initially possessed are excreted by ion exchange, so they are not involved in the bond formation stage. In other words, it is hard to say that the components of the catalyst are functioning at their fullest.

1.1.2 Asymmetric Intramolecular Ion Pair catalysis

On the other hand, in the case of intramolecular ion-pairing onium salts, in which anions and cations are covalently linked, both the anionic and cationic functions of the catalyst can be utilized. For example, when a basic anion-bearing onium salts is used as an organic base catalyst, nucleophilic anion species generated by deprotonation from a pronucleophile is expected to form tightly shaped pseudointramolecular ion pair with the onium salt by the cooperative function of ionic interaction and hydrogen bonding, which is advantageous for controlling subsequent bond formation step.

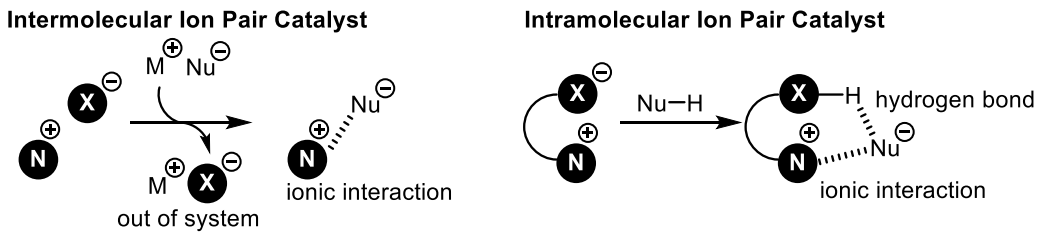

Figure 1 Inter- vs. intramolecular ion pair catalyst

Based on this strategy, our research group has developed intramolecular ammonium salts called ammonium betaines and its catalytic functions. In 2008, our group uncovered the ability to function as a chiral organic base catalyst through the development of a pseudo C_2-symmetric chiral quaternary ammonium aryl oxides. These betaines can be applied to the catalytic, highly enantioselective direct

Mannich-type reaction of α-nitrocarboxylates (Scheme 5).[6]

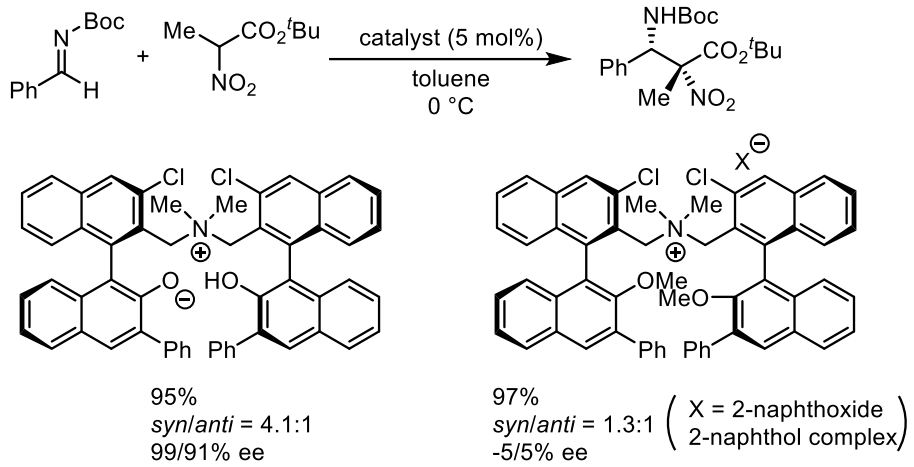

Scheme 5 Asymmetric Mannich-type reaction catalyzed by C2-symmetric chiral ammonium betaine

Although this report showed the capability of an intramolecular ion-pair catalyst, the pseudo C_2-symmetric chiral ammonium betaine has a high flexibility in its structure, which makes it difficult to clarify its three-dimensional structure by NMR analysis and X-ray diffraction, and it is not suitable for the design of precise asymmetric reaction fields. It was essential to understand the three-dimensional structure of the catalyst to promote further research based on the chemistry of chiral ammonium betaine. Structural modification of the catalyst was carried out with that in mind and a simplified C_1-symmetric chiral ammonium betaine was created as effective catalyst in the asymmetric Mannich-type reaction of α-nitrocarboxylates with *N*-Boc imines (Scheme 6).[7]

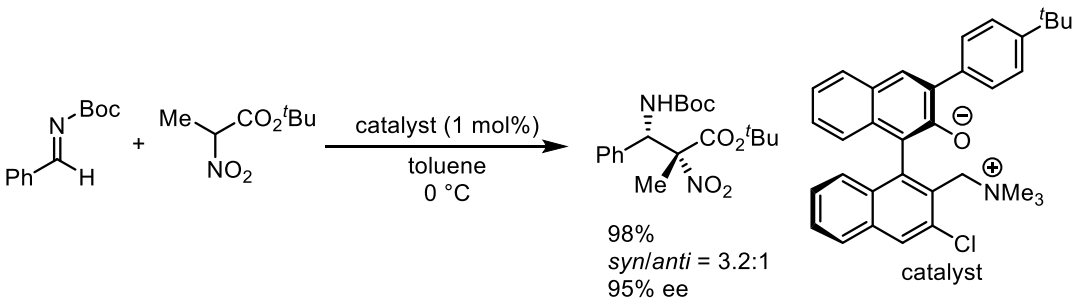

Scheme 6 Asymmetric Mannich-type reaction catalyzed by C1-symmetric chiral ammonium betaine

The structurally simplified C_1-symmetric chiral ammonium betaine exhibited high catalytic activity and enantioselectivity in nucleophilic addition reactions with various nucleophile precursors and *N*-Boc imines. For example, our group reported a stereoselective direct Mannich-type reaction of 2-alkoxythiazol-5(4*H*)-ones in 2010 (Scheme 7).[8] The Manncih adducts can be transformed to the

differently protected α-tetrasubstituted α,β-diamino acids and their derivatives easily and stereoselectively.

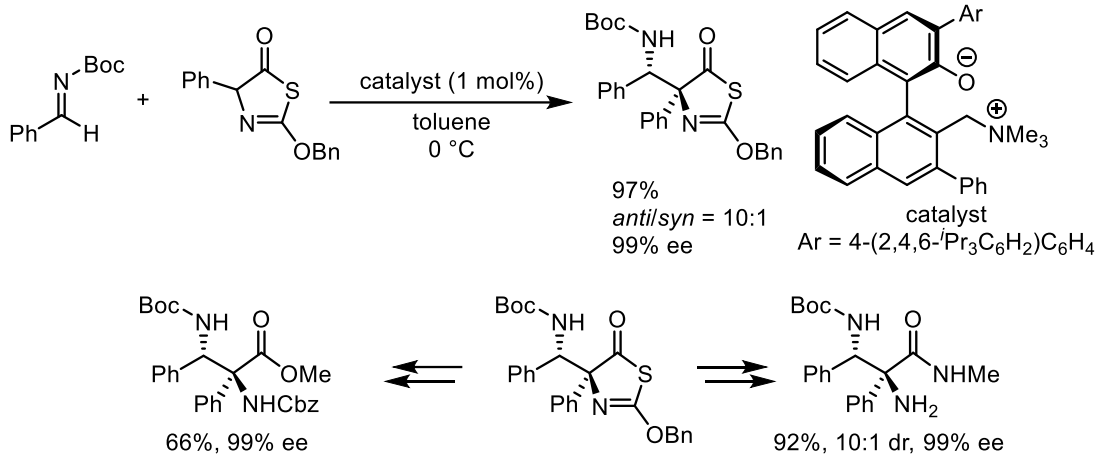

Scheme 7 Asymmetric Mannich-type reaction of thiazole-5(4H)-one

Subsequently, our group devised a strategy to utilize β,β-disubstituted nitroolefins as synthetically useful nucleophiles through the generation of corresponding vinylogous nitronate under the base catalysis of chiral ammonium betaines (Scheme 8).[9]

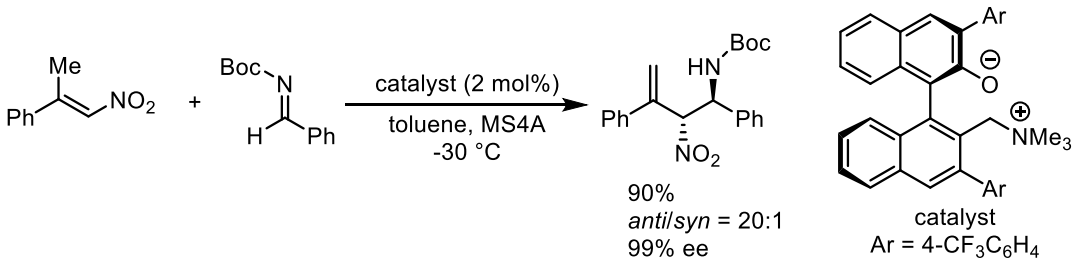

Scheme 8 Asymmetric aza-Henry reaction of β,β-disubstituted nitroolefins

Then, highly stereoselective aza-Henry reactions of nitro-substituted substrates as pronucleophile via (vinylogous) nitronates with aromatic imines were achieved under the catalysis of chiral ammonium betaines (Scheme 9,10).[10,11]

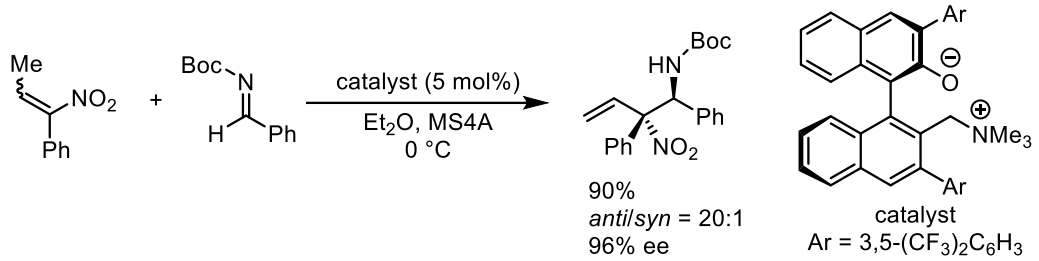

Scheme 9 Asymmetric aza-Henry reaction of α, β-disubstituted nitroolefins

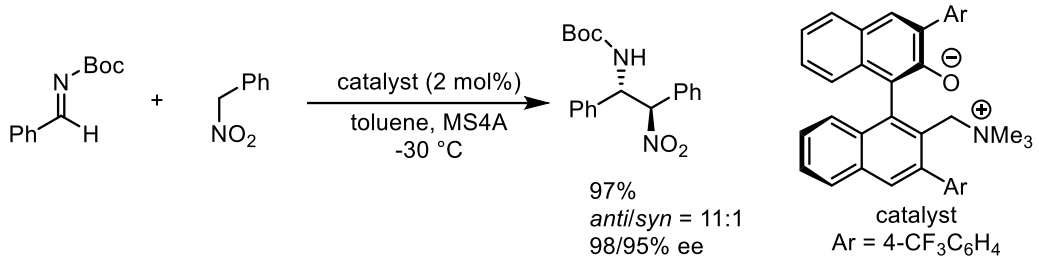

Scheme 10 Asymmetric aza-Henry reaction of substituted nirtomethanes

1.1.3 Chiral Ammonium Betaine-Catalyzed Asymmetric Mannch-type Reactions

In this context, we have been engaged in the development of asymmetric addition reactions using indoline alkaloids and quinolines as nucleophiles, which are structures often found in biologically active substances, and have developed asymmetric Mannich-type reaction systems for 3-aryloxindole and asymmetric Aza-Henry reaction systems for 3-nitrodihydroquinolones. Since the indoline skeleton possessing a C-3 quaternary asymmetric carbon is a structure commonly found in biologically active substances such as pharmaceuticals and natural products, the development of highly efficient and stereoselective methods for the synthesis of these compounds, especially catalytic molecular transformations, is an important issue. Among the various catalytic systems reported so far, the reaction of enolates as nucleophiles by the action of a base on oxindole having a highly acidic hydrogen atom at the C-3 carbon is one of the most versatile methods, and many effective catalysts for highly stereoselective conversion are known to be available. For example, Chen et al. achieved the first asymmetric Mannich-type reaction of oxindole using an acid-base cooperative thiourea catalyst. Maruoka et al. have reported a highly stereoselective Mannich-type reaction in a two-phase reaction system using a chiral phosphonium salt as a phase-transfer catalyst. Although these reports are excellent, there are some problems such as the lack of stereoselectivity when the substituent at position 3 is an aryl group and the limited application range of the substrate. In these circumstances, we discovered that the Mannich-type reaction of 3-aryloxindole with N-Boc imines proceeds in a highly stereoselective manner by utilizing chiral ammonium betaine as a catalyst.[12]

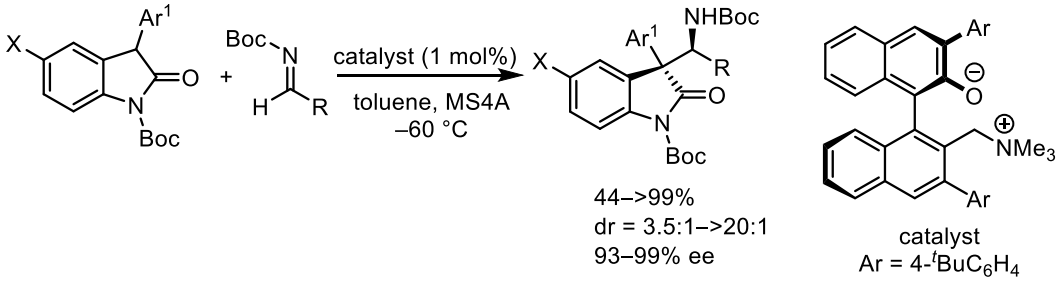

Scheme 11 Chiral ammonium betaine-catalyzed asymmetric Mannch-type reaction of oxindoles

Similarly, the hydroquinoline skeleton is a commonly found structure in natural products, and various methods have been developed to construct such a framework. The authors realized that the development of an enantioselective reaction using hydroquinoline as a nucleophile would lead to the development of a general method for the synthesis of hydroquinolines containing asymmetric carbons, and worked on the development of a reaction using a hydroquinolone with a nitro group as an activating group as a nucleophile.[13]

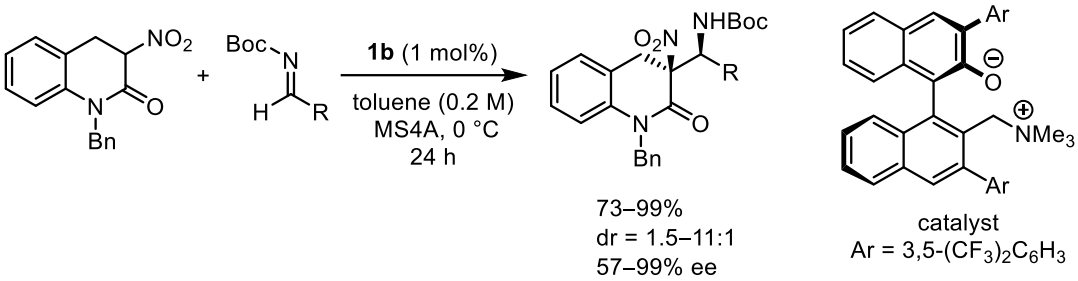

Scheme 12 Chiral ammonium betaine-catalyzed asymmetric Mannch-type reaction of quinlones

1.3.1 Cationic π-plane Compounds-Catalyzed Reactions via Single Electron Transfer

Radical reactions are one of the most fundamental molecular transformation in synthetic organic chemistry, and radical species have attracted much attention because of their unique and distinctive reactivity for a long time. It is known that compounds with a cationic π-plane, such as pyrylium and acridinium salts, have the ability to generate radical cationic species from organic compounds because the excited state produced by photo irradiation behaves as a strong one-electron oxidant. Recently, these molecules have attracted much attention and have been used in various organic syntheses because of their absorption wavelengths in the visible light region and the relatively long lifetimes of their excited states. For example, Nicewicz et al. reported a cyclization-endoperoxidation reaction system catalyzed by pyrylium salts, which was inspired by the photocyclization of dienes using dicyanoanthracene as a photo redox catalyst.[14] Acridinium salts also have high reduction potential in the excited state and work as strong oxidants.[15] For example, DiRocco and co-authors reported a decarboxylative Giese reaction using a structurally modified

acridinium salt as a photo-redox catalyst.[16]

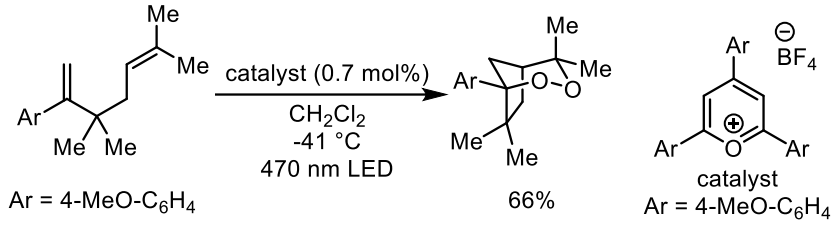

Scheme 13 Pyrylium salt-catalyzed photocyclization dienes

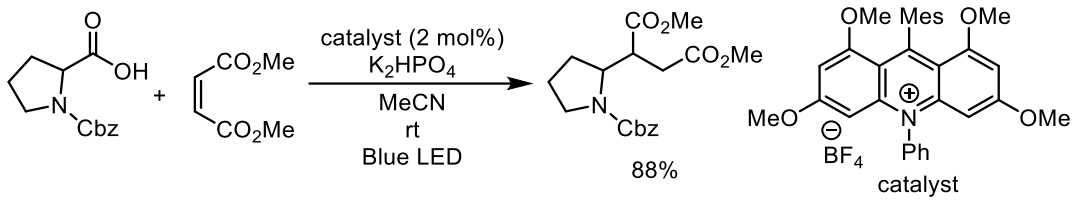

Scheme 14 Actidinium salt-cataluzed decarboxylative Giese reaction

1.3.2 Acridinium Betaine Catalyzed Homocoupling Reaction

The cation of ammonium betaine is important for the formation of ion-pairs with nucleophilic anionic species and the acquisition of high stereocontrol ability, but only the anionic moiety is responsible for the generation of reactive species. In other words, the cation site did not have the function to generate the reactive species. If the cation site is replaced to acridinium ion, which has a one-electron acceptor ability, it is expected to work in cooperative manner with the anion site to produce radical species by extracting hydrogen atoms from substrates with appropriate pKa and bond dissociation energy by the PCET mechanism.[17]

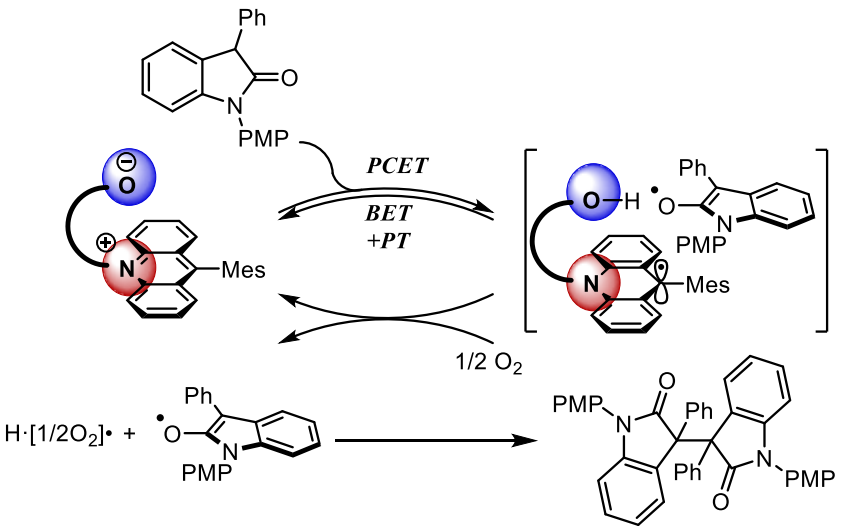

Figure 2 Plausible reaction mechanism of acridinum betaine-catalyed dimerization

In fact, it has been shown that acridinium betaine with acridinium ions and phenoxides can produce oxindole radicals by abstracting hydrogen atom at the 3-position of oxindole, which has a bond dissociation free energy of about 65 kcal/mol, and proceed with the dimerization reaction with high efficiency.[18]

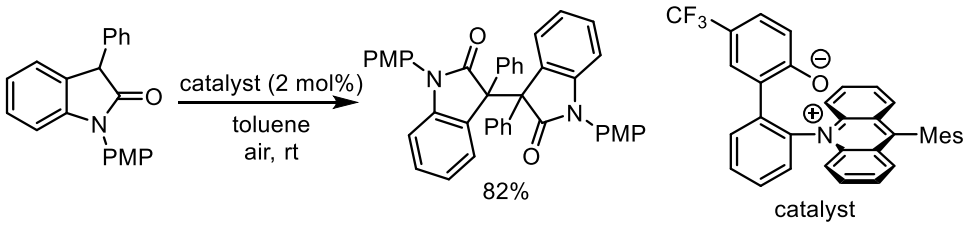

Scheme 15 Acridinum betaine-catalyed dimerization reaction of oxidoles

1.4 Dehydridative Transformation

Catalytic molecular transformation via carbanions, such as enolates generated through deprotonation with bases, has been widely used as the most basic bond formation methodology. However, the use of carbocations, which are complementary reactive species generated by hydride abstraction, for catalytic synthesis is extremely limited, and few nonmetallic catalysts are known to be effective for hydride abstraction. This is due to the fundamental problem that cationic species, which are the precursors of the products of the reaction triggered by hydride abstraction, tend to lose their cationic groups such as protons and produce molecules with unsaturated bonds, which are difficult to contribute to the catalytic regeneration by the transfer of hydride between molecules.

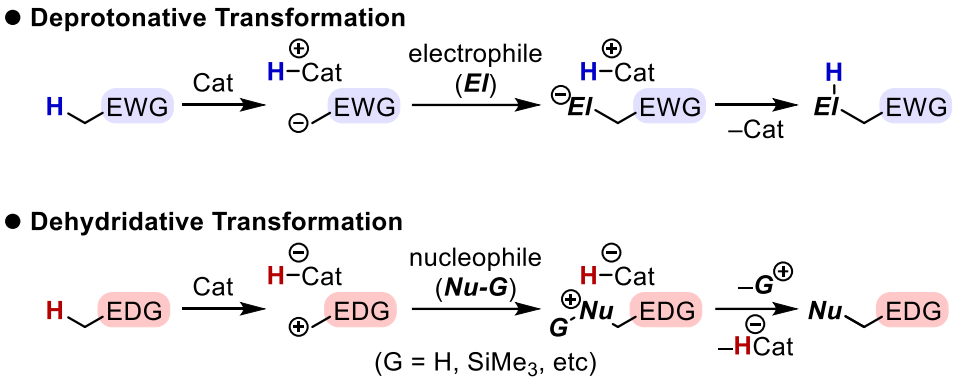

Figure 3 General schemes of deprotonative and dehydridative transformations

1.4.1 Dehydridation Activity of Triphenylmethylium Ion

The triphenylmethylium ion has long been known as a molecule that is able to abstract hydrogens from organic molecules as hydrides. For example, in 1976, Jung utilized triphenylmethylium ion to abstract hydride from the α-position of silyl-protected alcohols, and obtained aldehydes quantitatively by subsequent elimination of the silyl-protecting group.[19]

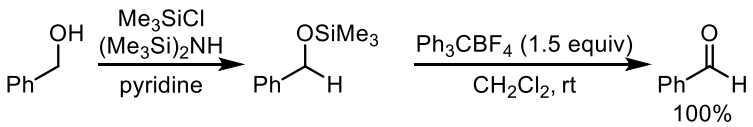

Scheme 16 Dehydridation of silyl-protected alcohol by triphenylmethylium ion

Lou, Liu and co-workers have also used trifluoroborate as a nucleophile to capture cations as an intermediate in the reaction and obtain carbon-carbon bond formed products in high yields.[20]

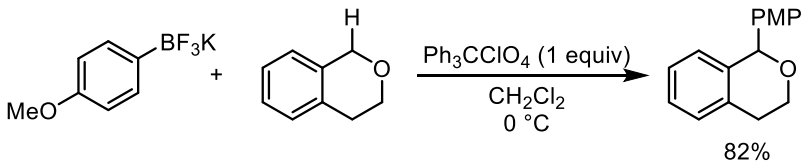

Scheme 17 Dehydridation-bond formation reaction reported by Lou and Liu

Since the triphenylmethane produced in this process is stable, it is difficult to regenerate the triphenylmethylium ion in the reaction system, and it is only used as a hydride abstracting agent in equal amounts to the substrate.

1.4.2 Quinone Type Molecule as Dehydridation Catalyst

2,3-Dichloro-5,6-dicyano-p-benzoquinone (DDQ), a quinone type molecule, has been used

as a molecule that can perform catalytic hydride extraction. While DDQ has high chemoselectivity, it is less electrophilic than triphenylmethylium ion, so its reaction efficiency varies greatly depending on the electronic state of the substrate, and it requires an equal or greater amount of metal oxide for catalyst regeneration.[21]

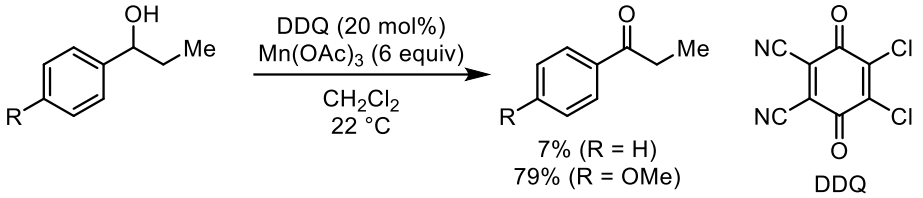

Scheme 18 DDQ-catalyed dehydridative transformation

1.4.3 Design and Development of *ortho*-Quinone Methide as Dehydridation Catalyst

Inspired by the hydride abstraction capabilities of triarylmethylium ions and the catalytic regeneration capabilities of quinone-type molecules, the author hypothesized that a molecule with the characteristics of both molecules could perform as a catalytic agent with high hydride abstraction capabilities. A zwitterionic molecule that contains a naphthoxide as the anionic moiety and a triarylmethylium ion as the cationic moiety can be considered as the canonical structure of quinone methides. The molecule produced by this zwitterionic molecule extracting a hydride from another molecule has a naphthoxide or naphthol that can be easily oxidized, and thus is expected to regenerate quinone methides by using an appropriate oxidant. In fact, it is known that quinone methides can be generated by the treatment of electron-rich phenol derivatives with silver oxide.[22]

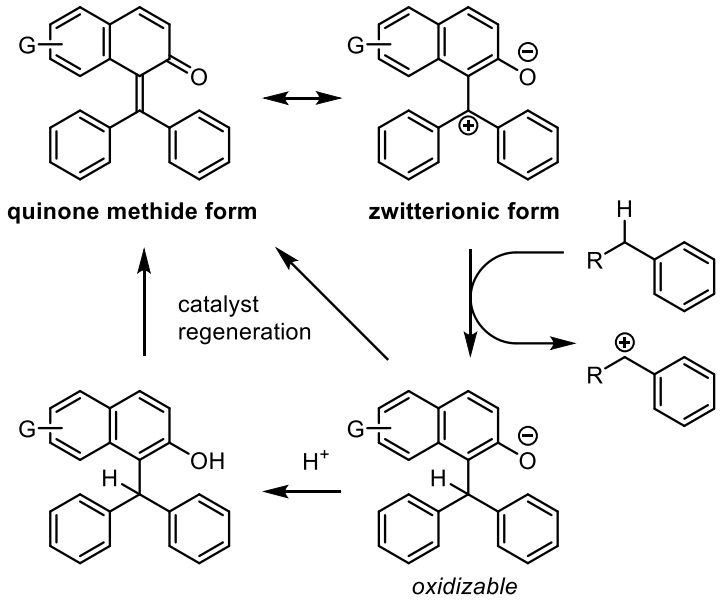

Figure 4 Concept of dehydridation catalyst

Based on this idea, we created *ortho*-hydroxytriarylmethane molecules that form quinone methides and reactive zwitterionic active species in the reaction system, and demonstrated their function as catalysts for hydride abstraction using benzyl alcohol as a model substrate.

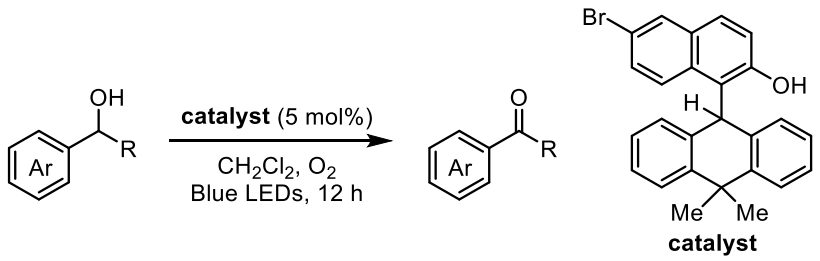

Scheme 19 Dehydridative oxidation of benzyl alcohol catalyzed by *o*-hydroxytriarylmethane

Summary

In these studies, the author developed the hydride abstraction catalysis of o-hydroxytriarylmethane via zwitterionic reactive species. He found that the catalysts work as good catalysts in the dehydridic oxidation of primary and secondary benzylic alcohols. In addition, he provided computational insights into the photochemical behavior of the newly developed catalysts and the reaction intermediates.

Reference

(1) Dolling, U.-H.; Davis, P.; Grabowski, E. J. J. *J. Am. Chem. Soc.*, **1984**, *106*, 446.

(2) Corey, E. J.; Xu, F.; Noe, M. C. *J. Am. Chem. Soc.*, **1997**, *119*, 12414.

(3) Lygo, B.; Wainwright, P. G. *Tetrahedron Lett.*, **1997**, *38*, 8595.

(4) Ooi, T.; Kameda, M.; Maruoka, K. *J. Am. Chem. Soc.*, **1999**, *121*, 6519.

(5) (a) Ooi, T.; Maruoka, K. *Angew. Chem. Int. Ed.*, **2007**, *46*, 4222. (b) Hashimoto, T.; Maruoka, K. *Chem. Rev.*, **2007**, *107*, 5656.

(6) Uraguchi, D.; Koshimoto, K.; Ooi, T. *J. Am. Chem. Soc.*, **2008**, *130*, 10878.

(7) Uraguchi, D.; Koshimoto, K.; Sanada, C.; Ooi, T. *Tetrahedron Asymmetry*, **2010**, *21*, 1189.

(8) Uraguchi, D.; Koshimoto, K.; Ooi, T. *Chem. Commun.*, **2010**, *46*, 300.

(9) Uraguchi, D.; Oyaizu, K.; Ooi, T. *Chem. Eur. J.*, **2012**, *18*, 8306.

(10) Oyaizu, K.; Uraguchi, D.; Ooi, T. *Chem. Commun.*, **2015**, *51*, 4437.

(11) Uraguchi, D.; Oyaizu, K.; Ooi, T. *Chem. Asian. J.*, **2015**, *10*, 334.

(12) Torii, M.; Kato, K.; Uraguchi, D.; Ooi, T. *Beilstein J. Org. Chem.* **2016**, *12*, 2099.

(13) Uraguchi, D.; Torii, M.; Kato, K.; Ooi, T. *Heterocycles* **2017**, *94*, 441.

(14) Gesmundo, N. J.; Nicewicz, D. A. *Beilstein J. Org. Chem.* **2014**, *10*, 1272.

(15) Fukuzumi, S.; Kotani, H.; Ohkubo, K.; Ogo, S.; Tkachenko, N. V.; Lemmetyinen, H. *J. Am. Chem. Soc.* **2004**, *126*, 1600.

(16) Joshi-Pangu, A.; Lévesque, F.; Roth, H. G.; Oliver, S. F.; Campeau, L.-C.; Nicewicz, D.; DiRocco, D. A. *J. Org. Chem.* **2016**, *81*, 7244.

(17) For reviews on PCET, see: (a) Huynh, M. H. V, Meyer, T. J. *Chem. Rev.* **2007**, *107*, 5004. (b) Weinberg, D. R.; Gagliardi. C. J.; Hull, J. F.; Murphy, C. F.; Kent, C. A.; Westlake, B. C.; Paul, A.; Ess, D. H.; McCafferty, D. G.; Meyer, T. J. *Chem. Rev.* **2012**, *112*, 4016. (c) Yayla, H. G.; Knowles, R. R. *Synlett* **2014**, *25*, 2819. (d) Gentry, E. C.; Knowles, R. R. *Acc. Chem. Res.* **2016**, *49*, 1546.

(18) Uraguchi, D.; Torii, M.; Ooi, T. *ACS Catal.* **2017***, 7,* 2765-2769

(19) Jung, M. E. *J. Org. Chem.* **1976**, *41*, 1479.

(20) Chen, W.; Xie, Z.; Zheng, H.; Lou, H.; Liu, L. *Org. Lett.* **2014**, *16*, 5988.

(21) Cosner, C. C.; Cabrera, P. J.; Byrd, K. M.; Thomas, A. M. A.; Helquist, P. *Org. Lett.* **2011**, *13*, 2071.

(22) Bishop, L. M.; Winkler, M.; Houk, K. N.; Bergman, R. G.; Trauner, D. *Chem. Eur. J.* **2008**, *14*, 5405.

Chapter 2

Design and Characterization of *o*-Hydroxytriarylmethane as a Hydride Abstraction Catalyst

Abstract

An *o*-quinone methide (*o*-QM) featuring an overcrowded olefinic framework is introduced, which exhibits dehydridation activity owing to its enhanced zwitterionic character, particularly through photoexcitation. An experimental analysis and density functional theory calculations provide mechanistic insights; the ground-state zwitterionic intermediate abstracts a hydride and proton simultaneously, and the active oxygen species facilitate catalyst regeneration.

Introduction

Triarylmethylium ions are one of the most stable carbocations because of the delocalization of the positive charge on the three aromatic rings, and they play an important role in organic chemistry (Figure 1).[1] Triarylmethylium ions are readily yielded from the corresponding alcohols or ethers by treating them with acid catalysts. This characteristic allows the triarylmethyl group to be suited as a protecting group not only for hydroxyl groups but also for other heteroatom-containing functional groups.[2] In fact, the triarylmethyl protection can be applied in various fields of organic and bioorganic chemistry, including nucleoside, oligonucleotide, peptide, and carbohydrate chemistry. When a substituent of oxygen or nitrogen is present in the *para*- or *ortho*-position of the aromatic unit of the triarylmethylium ion, the cation has the propensity to isomerize into the quinoid form. The quinoid form is a major structural component of organic dyes such as rosolic acid and malachite green, and xanthene phosphors such as fluorescein and rhodamine. Furthermore, the parent triarylmetylium ion and its derivatives are isoelectronic with triarylboranes and can accept an electron pair into their low-lying empty p-orbital, thus exhibiting Lewis acidity.[3] This allows not only the activation of Lewis bases but also hydride abstraction (dehydridation). The latter is a remarkable property of the triarylmethylium ions, since organic molecules capable of dehydridation are very rare.[4]

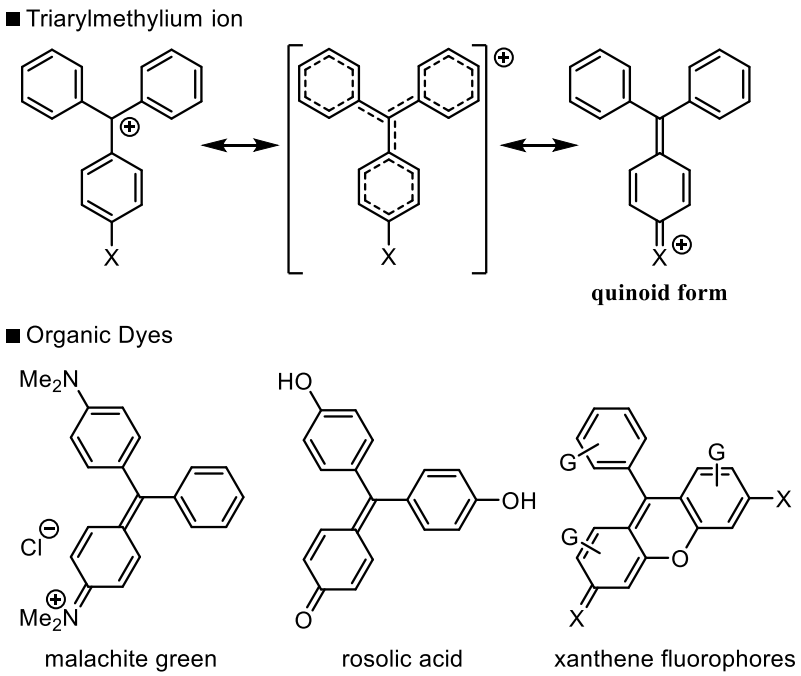

Figure 1 Triarylmethylium derivatives (X = O, NR_2)

Compared to base-promoted deprotonative reactions, transformations via dehydridation reactions have not been well studied. The reason for this lies in the fact that there are few dehydridating reagents available, and the organic molecules exerting dehydridation activity are virtually limited to triarylmethylium ions and quinones.[5,6] Furthermore, although the dehydridative oxidation of functional groups containing heteroatoms, such as alcohols and amines, via the generation of cationic species is a powerful tool for selective manipulation of functional groups, the development of a catalytic system remains a major challenge due to the difficult in regenerating dehydridating

reagents.[7] Upon dehydridation, dehydridating reagents are typically converted into reduced forms such as triarylmethane and hydroquinone, and re-oxidation to the active form often requires stoichiometric excesses of strong oxidants, which can lead to degradation of substrates and products.[5a] Although several systems for regenerating quinones as dehydridating reagents with metal catalysts have been reported, the development of regenerable dehydridation reagents has not been successful. In this study, we designed a molecule to impart regenerability to triarylmethylium ions, which enabled the dehydridative oxidation of benzylic alcohols under mild and operationally simple conditions.

Results and Discussion

To design a dehydridation catalyst, we hypothesized that regeneration process could be favored by increasing the stability of the triarylmethylium ion through devising the molecular structure. As generally recognized, introducing an electron-donating group to one of the aromatic rings of a triarylmethylium ion stabilizes the cation through the formation of a quinoid structure. In other words, one of the canonical structures of a quinone methide (QM) containing two aromatic substituents on the terminal sp^2 carbon can be regarded as a surrogate for triarylmethylium ion.[8] However, while QM is known to have a very high electrophilicity and undergoes nucleophilic conjugate addition at the partially cationic benzylic carbon, the contribution of the zwitterionic resonance form with triarylmethylium and aryloxide moieties is considered to be infinitely small.[9] Based on these characteristics in mind, we reasoned that we could elicit dehydridation activity by providing QMs with molecular distortion that would weaken the conjugation of the carbonyl and olefin functional groups. To this end, we sought to introduce an overcrowded olefinic component[10] into the QM framework, effectively disrupting the conjugation by interfering with the inherent planarity, and employed type A *ortho*-QM (*o*-QM) as the primary structural platform to access triarylmethylium ions with catalytic capability (Figure 2).

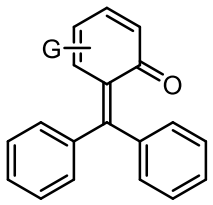

A
ortho-quinone methide

Figure 2 *o*-QM having overcrowded olefinic component.

We evaluated the validity of our hypothesis by characterizing the intrinsic reactivity of isolable *o*-QM **1** derived from 2-naphthol toward an organic hydride donor (Figure 3a).[11]

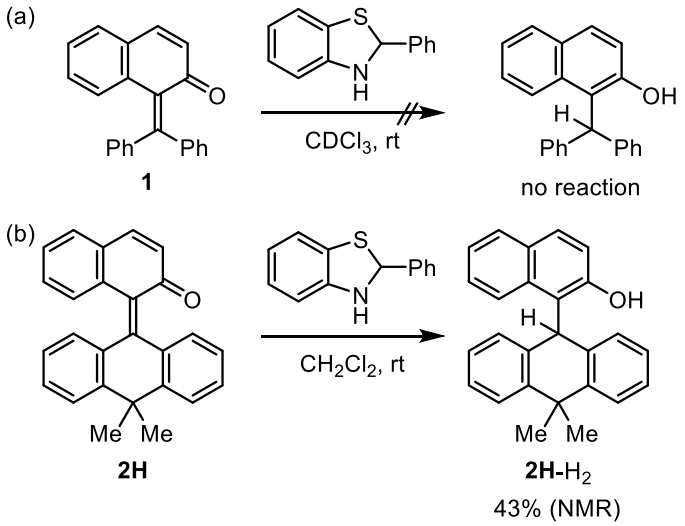

Figure 3 Reduction of *o*-QMs **1** and **2** with 2-phenyl benzothiazoline.

Therefore, **1** was treated with an equimolar amount of 2-phenyl benzothiazoline[12] in $CDCl_3$ at ambient temperature, and ^{1}H NMR analysis of the resulting reaction mixture showed no 1,4-reduction had occurred. We speculated that the lack of reactivity of 1 might be due to the insufficient cationic nature of the *β*-carbon. We therefore prepared *o*-QM **2H** with a 10,10-dimethyl-9(10*H*)-anthracenylidene framework, hypothesizing that the larger steric hindrance around the olefinic core would induce a conformational distortion that would be effective in weakening the conjugation with the carbonyl group (Figure 3b). In fact, treatment of **2H** with 2-phenyl benzothiazoline yielded the 1,4-reduction to give **2H**-H_2 in a moderate yield, suggesting that the zwitterionic nature of **2H** has been anhanced. In order to clarify the origin of the difference in reactivity between **1** and **2H**, we first performed spectroscopic analysis. However, the difference between the maximum absorption wavelengths of **1** and **2H** was almost negligible, indicating that their effective conjugation length and degree of zwitterionic character should be similar (Figure 4).

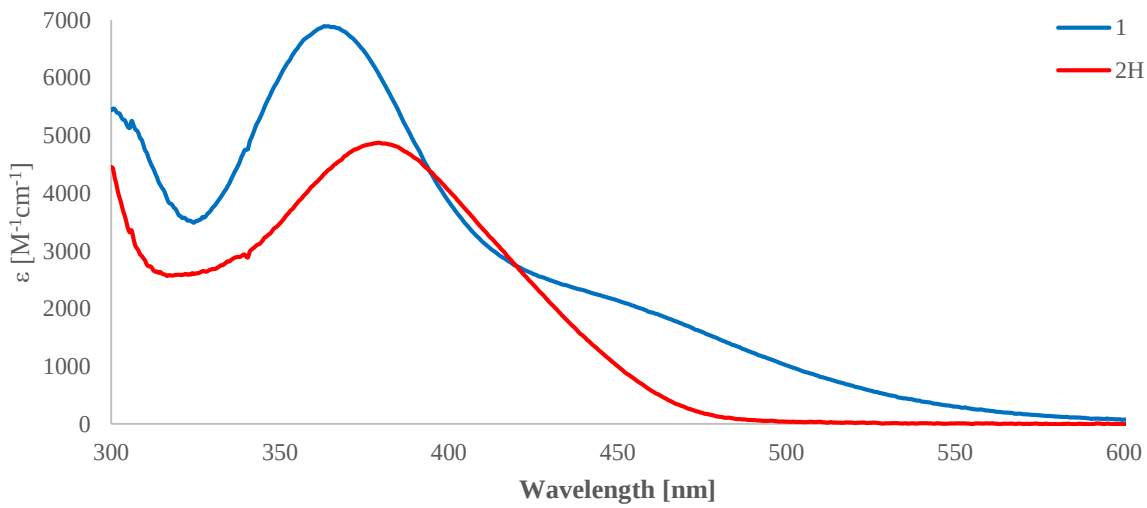

Figure 4 Absorption spectra of *o*-QMs **1** and **2H**

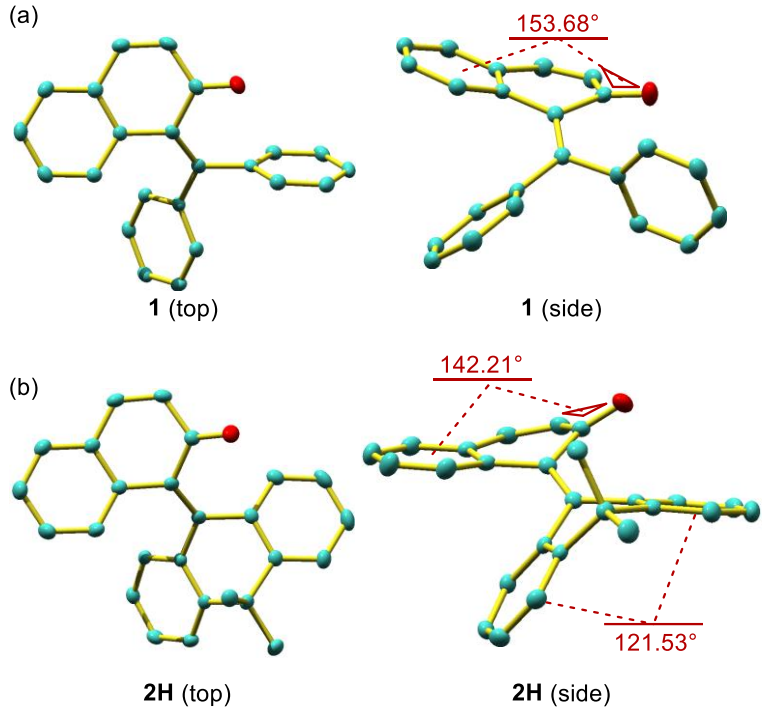

Figure 5 ORTEP diagrams (Calculated hydrogens were omitted for clarity. Thermal ellipsoids are displayed at 50% probability level.) of (a) **1** and (2) **2H**.

Subsequent single-crystal X-ray diffraction analysis also revealed that **1** and **2H** have almost same anti-folded structures around the *α*,*β*-unsaturated carbonyl moiety, but the mean plane dihedral angle of the benzocyclohexadienone subunit (142.21°) was much smaller than that of 1 (153.68°), indicating a significant distortion was observed (Figure 5a and b). In addition, the dihydroanthracene subunit of **2H** was bent significantly (121.53°) to minimize the steric repulsion between the substituents on the olefinic carbons in the fjord region. These distorted structures can be reproduced by simulations using density functional theory (DFT) calculations (SMD(CH_2Cl_2)-CAMB3LYP/6-31+G(d) level),[13] indicating that the distortions in the crystal structure are not derived from the crystal packing force. Based on these results and the computationally optimized structure of **2H**-H_2, which is composed of planar 2-naphthol and dihydroanthracene subunits, the dehydridation activity of **2H** can be attributed to strain release through hydride acceptance. However, this degree of distortion was not sufficient to increase the contribution of the zwitterionic resonance form to an extent that **2H** would abstract a hydride from less reactive donors such as cyclohexa-1,4-diene (Figure 6a).

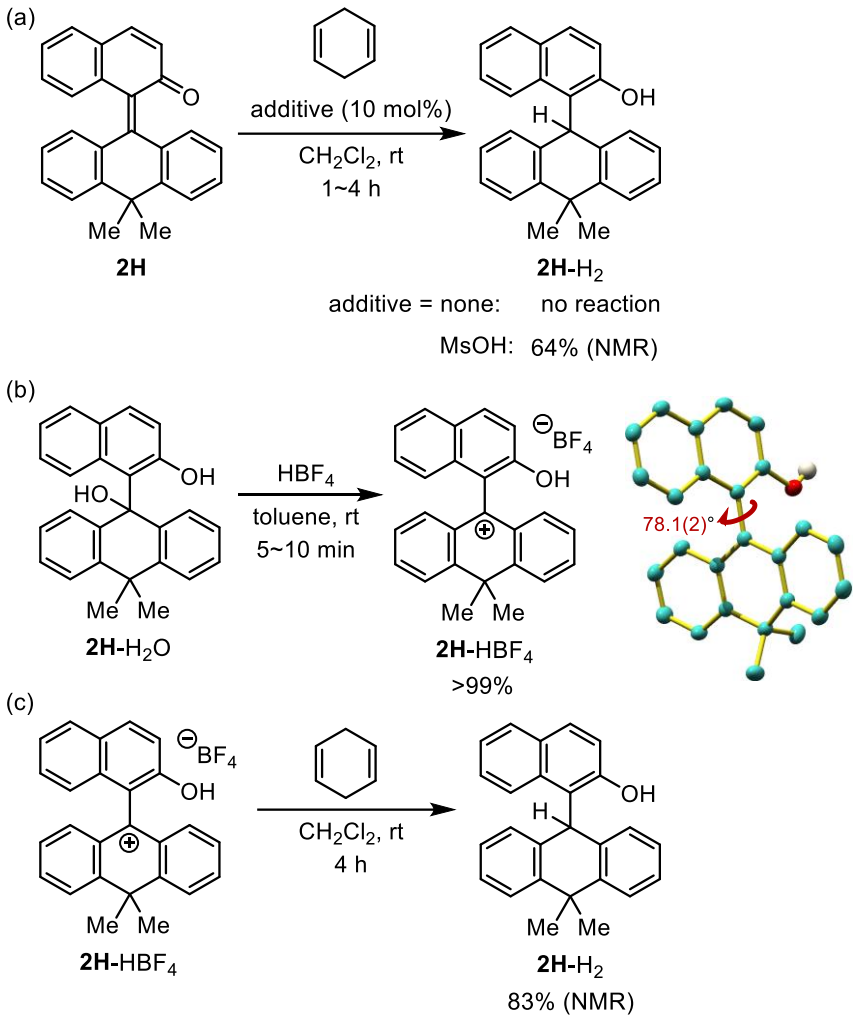

Figure 6 (a) Reduction of **2H** with cyclohexa-1,4-diene. (b) Preparation and ORTEP diagram of **2H**-HBF_4 (Calculated hydrogens and BF_4^- were omitted for clarity. Thermal ellipsoids are displayed at 50% probability level.). (c) Reduction of **2H**-HBF_4 with cyclohexa-1,4-diene.

This interpretation is consistent with the observation that the addition of a catalytic amount of methanesulfonic acid (MsOH) to the reaction of **2H** with cyclohexa-1,4-diene promoted the production of **2H-H$_2$** at ambient temperature. This is considered to be due to the increased intervention of the zwitterionic structure in its protonated, carbocationic form. The generation of this intermediate was confirmed by the color change of the reaction solution from pale yellow to deep red upon the introduction of MsOH. The reddish color was indicative of carbocationic character, and X-ray diffraction analysis of the deep-red single crystal of **2H**-HBF_4 prepared separately from **2H**-H_2O and HBF_4 revealed its three-dimensional structure bearing a benzylic carbocation (Figure 6b). The nearly vertically connected 2-naphthol and dihydroanthracene subunits (torsion angle: 78.1°) were both planar, meaning that the structural distortion of the precursor **2H** was completely released. The benzylic carbon adopts a sp^2-hybridized planar structure (sum of the angles: 360°) according to its cationic nature and show high reactivity, as demonstrated by the smooth reaction of **2H** with cyclohexa-1,4-diene to give **2H**-H2 in 83% yield (Figure 6c). Since the participation of the zwitterionic form was of critical relevance to the operation of the dehydridation process, we investigated possibility of generating the zwitterionic form without the use of acidic additives. As it is known that

overcrowded olefins with an anti-folded structure form biradicals and twist around the C=C bond axis upon photoexcitation,[14] we hypothesized that *o*-QM **2H** with a push-pull-type structure could be converted into the zwitterionic resonance form upon photoexcitation via intramolecular charge-transfer state with concurrent molecular motion. The validity of this hypothesis was assessed by the investigating the photoexcitation process of **2H** using time-dependent density functional theory (TD-DFT) calculations (SMD(CH_2Cl_2)-TD-CAMB3LYP/6-31+G(d) level) (Figure 6).

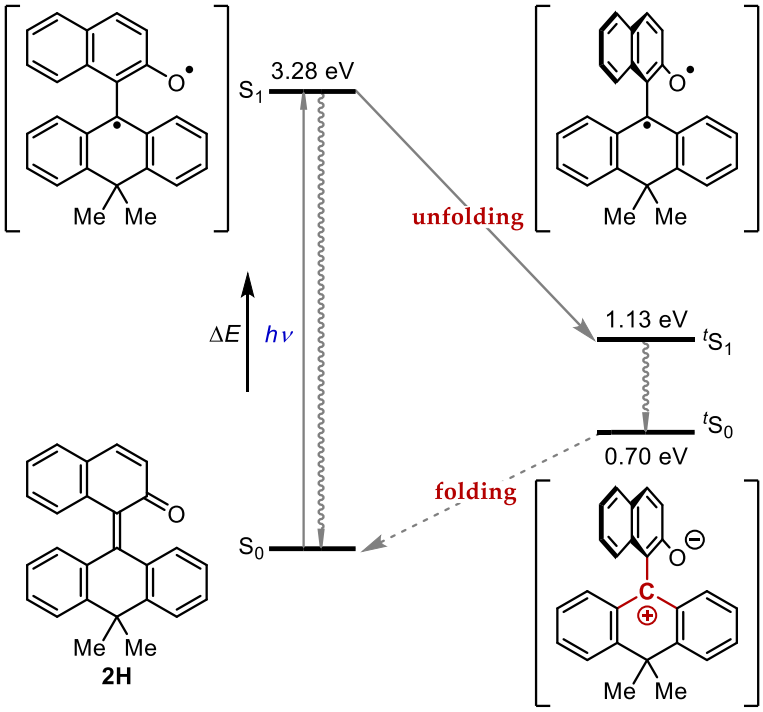

Figure 7 Jablonski diagram of **2H**

After the local excitation of the ground state of **2H** (S_0), the lowest first singlet excited state (S_1) (ΔE = 3.28 eV) is obtained through vibrational relaxation and internal conversion. Since the double-bond nature of the overcrowded olefinic core is disrupted with the formation of the biradical, the structural distortion in the S_1 state with the anti-folded conformation is spontaneously released via the unfolding process. As a result, the twisted S_1 ($^tS_1$) state, in which the two subunits are vertically connected, is 2.15 eV more stable than parent S_1. Finally, the zwitterionic form of **2H** ($^tS_0$) required to act as the dehydridating reagent is afforded by the relaxation of $^tS_1$, which is expected to be rapid because of the small energy gap (ΔE = 0.43 eV) between $^tS_1$ and $^tS_0$. The calculated molecular orbitals of $^tS_0$ showed intramolecular charge separation, with the largest orbital lobe LUMO located on the benzylic carbon, reflecting the zwitterionic nature of $^tS_0$ (Figure 8).

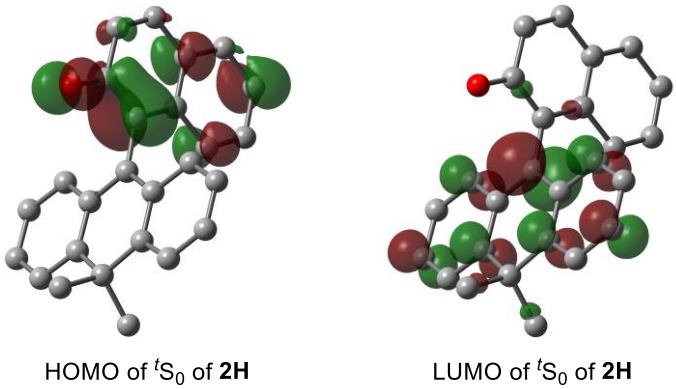

Figure 8 Frontier orbitals of $^tS_0$ of **2H**

The similarity of the structures of **2H**-HBF_4 and $^tS_0$ calculated at the SMD(CH_2Cl_2)-TD-CAMB3LYP/6-31+G(d) level indicates that the cationic nature of the benzylic carbon in the zwitterionic form of **2H** is important for obtaining the dehydridation reactivity. Although the refolding from $^tS_0$ (ΔE = 0.70 eV) to S_0 is thermodynamically favorable, it requires a two-step transition process after the structural relaxation to obtain **int1**, as seen in Figure 8. That is, to obtain **int2**, the dihydroanthracene subunit is bent along the C9-C10 axis to increase the double-bond character of the bridging bond, and then rotated around the bridging bond.

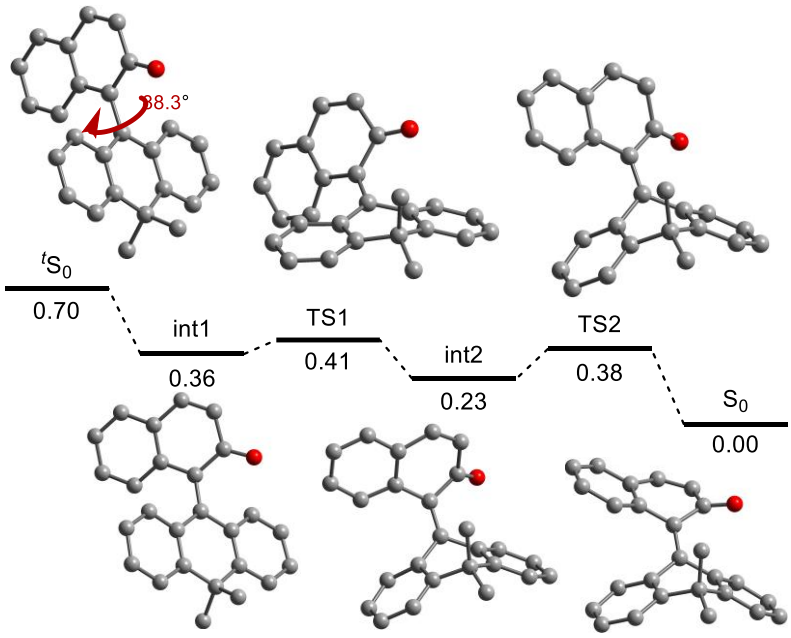

Figure 9 Re-folding process from $^tS_0$ to S_0

Although the energetic barriers for the two transition states (**TS1** and **TS2**) were estimated to be very low, the profile of the transition process suggests that the lifetime of $^tS_0$ could participate in the intermolecular dehydridation reaction. Based on these computational analyses, we experimentally investigated the possibility of generation of the zwitterionic form of **2H** by irradiation of a mixture of **2H** and cyclohexa-1,4-diene in dichloromethane at ambient temperature, and yielded **2H**-H_2 in 56% yield (Scheme 1).

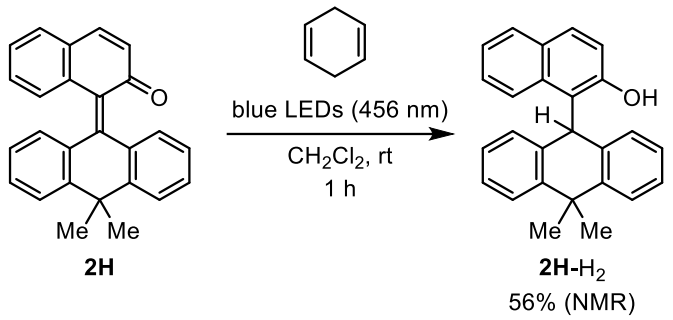

Scheme 1 Reduction of **2H** with cyclohexa-1,4-diene under photoirradiation

Next, to complete the catalytic cycle, based on the fact that photoirradiation was effective for the generation of the zwitterionic form of **2H**, we investigated the conditions for the regeneration of **2H** from the reduced form **2H**-H_2. As a result, we found that the hydrate form **2H**-H_2O was obtained by photoirradiation of **2H**-H_2 under an oxygen atmosphere (Scheme 2, indicating the applicability of quinone methide **2H** as a dehydridation catalyst..

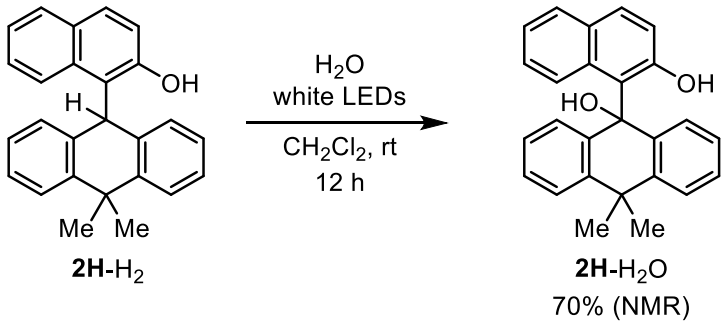

Scheme 2 Oxidation of **2H**-H_2 under photoirradiation

Conclusion

We have demonstrated the feasibility of exploiting the potential reactivity of *o*-QMs as a dehydridation reagent. The contribution of the zwitterionic resonance form of *o*-QM can be enhanced by introducing an overcrowded olefinic framework, and its dehydridation activity can be fully realized by photoexcitation. We expect that this study stimulates further research into the possibility of utilizing dehydridative reactions in synthetic organic chemistry.

General Information:

Infrared spectra were recorded on a SHIMADZU IRAffinity-1 spectrometer. UV-Vis absorption spectra were recorded on a Shimadzu UV-1800 spectrometer. ^{1}H NMR spectra were recorded on a JEOL JNM-ECZ400S (400 MHz), JEOL JNM-ECA500II (500 MHz), or JEOL JNM-ECA600II (600 MHz) spectrometer. Chemical shifts are reported in ppm from the solvent resonance (CD_3CN: 1.94 ppm, C_6D_6: 7.16 ppm) or tetramethylsilane (0.00 ppm; $CDCl_3$) resonance as the internal standard. Data are reported as follows: chemical shift, integration, multiplicity (s = singlet, d = doublet, t = triplet, m = multiplet, br = broad, brd = broad-doublet), and coupling constants (Hz). ^{13}C NMR spectra were recorded on a JEOL JNM-ECA600II (151 MHz) spectrometer with complete proton decoupling. Chemical shifts are reported in ppm from the solvent resonance ($CDCl_3$: 77.16 ppm, CD_3CN: 1.32 ppm, C_6D_6: 128.06 ppm). ^{19}F NMR spectra were recorded on a JEOL JNM-ECZ400S (376 MHz) spectrometer with complete proton decoupling. Chemical shifts are reported in ppm from benzotrifluoride (–64.0 ppm) resonance as the external standard. The high-resolution mass spectrometry were conducted on Thermo Fisher Scientific Exactive (ESI). Analytical thin layer chromatography (TLC) was performed on Merck precoated TLC plates (silica gel 60 F_{254}, 0.25 mm). Flash column chromatography was performed on Silica gel 60N (spherical neutral, 40-50 μm; Kanto Chemical Co., Inc.). Simple chemicals were purchased and used as such.

Experimental Section:

Procedures for Reduction of 2H and 2H-HBF$_4$ with Organic Hydride Sources:

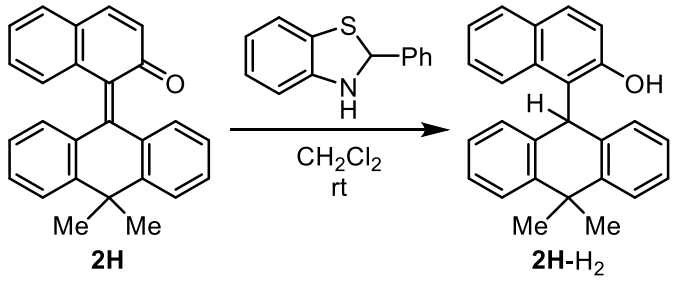

2H (3.48 mg, 0.010 mmol) was treated with 2-phenylbenzothiazoline (2.56 mg, 0.012 mmol) in CH_2Cl_2 (1.0 mL) at room temperature for 3 h. The reaction mixture was concentrated and the chemical yield of **2H**-H_2 was determined to be 43% by ^{1}H NMR analysis (400 MHz) using trimethylsilylbenzene as an internal standard.

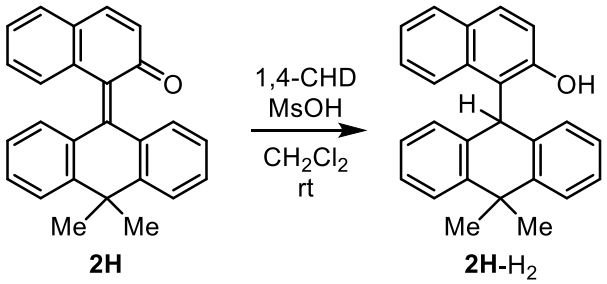

To a solution of **2H** (3.48 mg, 0.010 mmol) and cyclohexa-1,4-diene (1,4-CHD, 4.7 μL, 0.050 mmol) in CH_2Cl_2 (1.0 mL) was added a 1.0 M solution of methanesulfonic acid (MsOH) in CH_2Cl_2 (1.0 μL, 0.0010 mmol), and the resulting solution was stirred at room temperature for 4 h. After concentration, the chemical yield of **2H**-H_2 was determined to be 64% by ^{1}H NMR analysis (400 MHz) using trimethylsilylbenzene as an internal standard.

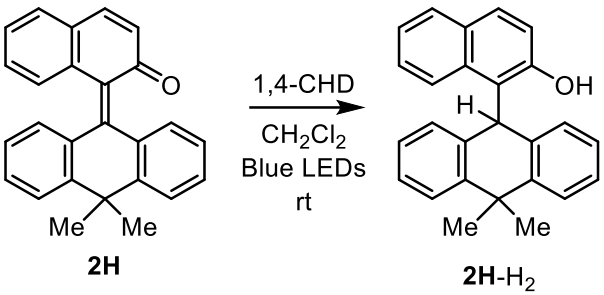

A solution of **2H** (3.48 mg, 0.010 mmol) and 1,4-CHD (4.7 μL, 0.050 mmol) in CH_2Cl_2 (1.0 mL) was irradiated with Kessil PR160L-456 Blue LED lamps (456 nm) with fans under argon atmosphere for 1 h. The reaction mixture was concentrated under reduced pressure for determining chemical yield of **2H**-H_2 to be 56% by ^{1}H NMR analysis (400 MHz) using trimethylsilylbenzene as an internal standard.

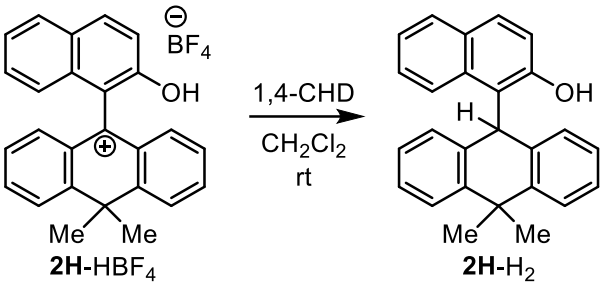

To a solution of **2H**-HBF_4 (4.36 mg, 0.010 mmol) in CH_2Cl_2 (1 mL) was added 1,4-CHD (4.7 μL, 0.050 mmol) at room temperature. After 4 h of stirring, the reaction mixture was concentrated and the ^{1}H NMR analysis of the crude residue using trimethylsilylbenzene as an internal standard determined the chemical yield of **2H**-H_2 to be 83%.

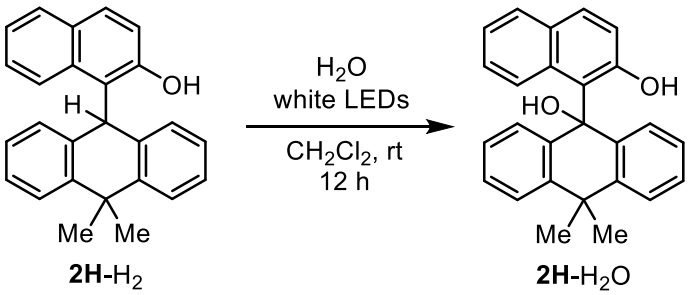

To a solution of **2H**-H_2 (3.50 mg, 0.010 mmol) in CH_2Cl_2 (1 mL) was irradiated with white LEDs under oxygen atmosphere for 12 h. The reaction mixture was concentrated under reduced pressure for determining chemical yield of **2H**-H_2O to be 70% by ^{1}H NMR analysis (400 MHz) using trimethylsilylbenzene as an internal standard.

Absorption Spectroscopy:

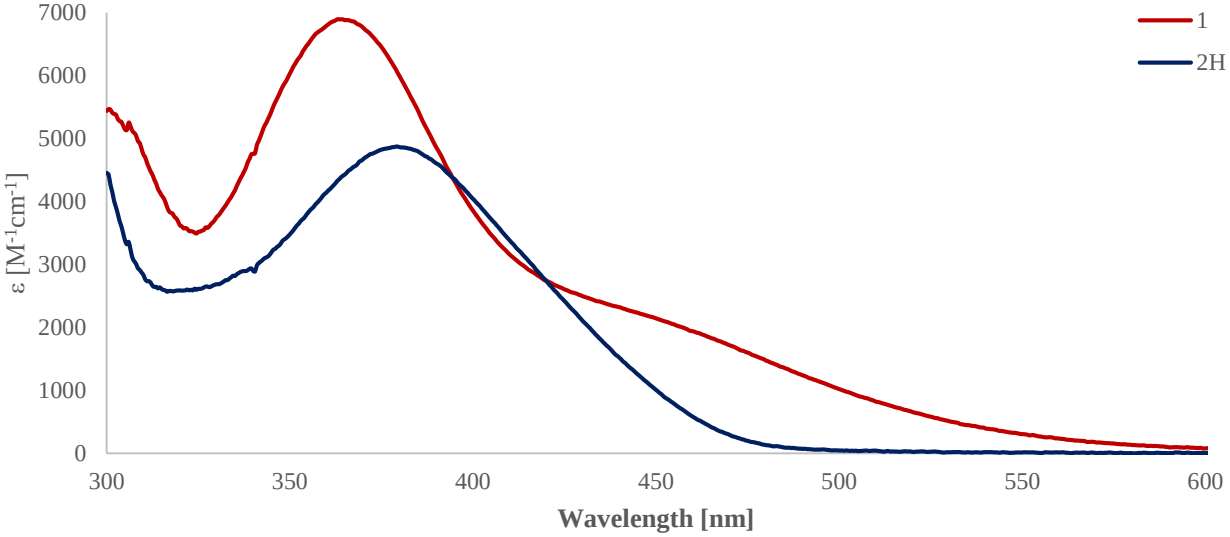

Figure S1. Absorption spectra of **1** and **2H** in CH_2Cl_2 at room temperature.

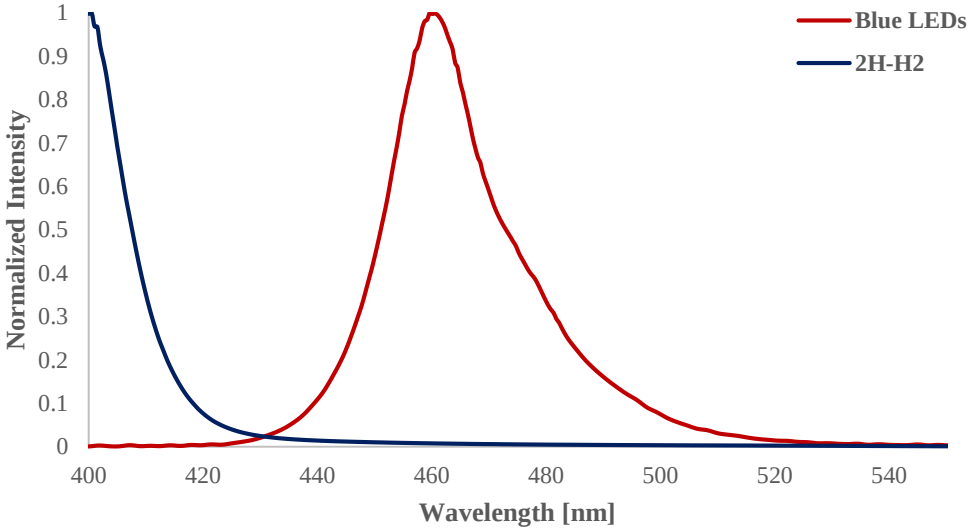

Figure S2. Absorption spectrum of **2H**-H_2 in CH_2Cl_2 and irradiation spectrum of Kessil PR160L-456 Blue LED lamp.

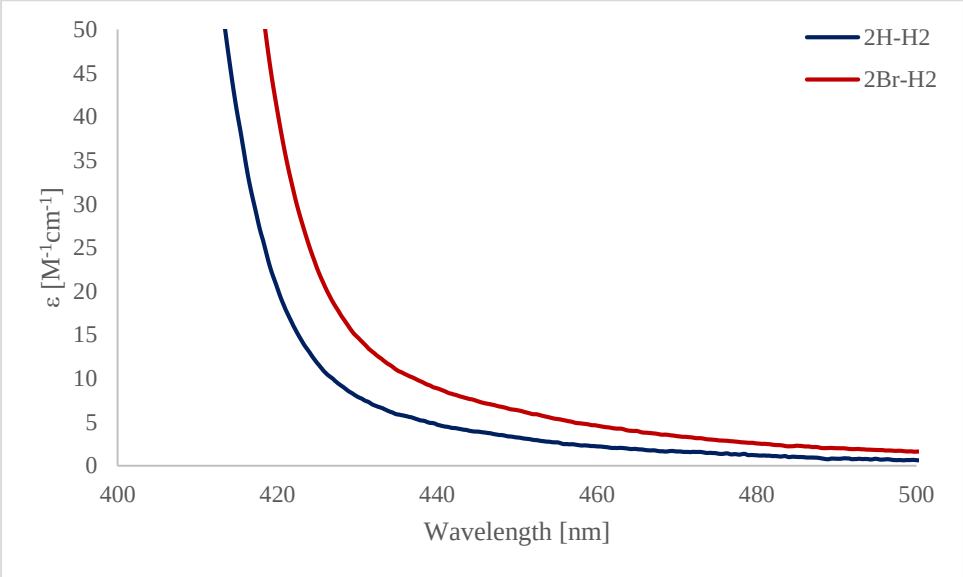

Figure S3. Absorption spectra of **2H**-H_2 and **2Br**-H_2 in CH_2Cl_2 at room temperature.

Synthesis and Characterization of Quinone Methides and Their Precursors:

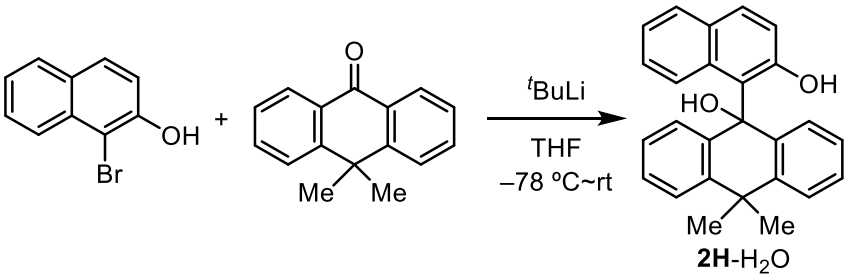

Preparation of 9-(2-hydroxynaphthalen-1-yl)-10,10-dimethyl-9,10-dihydroanthracen-9-ol (2H-H_2O): To a solution of 1-bromo-2-naphthol (1.8 g, 8.0 mmol) in anhydrous tetrahydrofuran (THF) (27.0 mL) was added ^{t}BuLi (1.6 M in ^{n}pentane, 15.0 mL, 24.0 mmol) dropwise at –78 °C and the reaction mixture was stirred at –15 °C for 1 h. A solution of 10,10-dimethylanthrone (1.7 g, 7.5 mmol) in anhydrous THF (8.0 mL) was introduced dropwise to the mixture at –78 °C. The resulting mixture was allowed to warm to room temperature and stirred there for overnight. The reaction mixture was poured into a saturated aqueous solution of NH_4Cl and extracted with ethyl acetate (EA) three times. The combined organic extracts were washed with brine and dried over Na_2SO_4. After removal of volatiles under reduced pressure, purification of the residue was performed by column chromatography on silica gel (hexane (H)/EA = 10:1 as eluent) to afford **2H**-H_2O in 77% yield (2.11 g, 5.8 mmol) as a white solid. **2H-H_2O:** ^{1}H NMR (600 MHz, $CDCl_3$) δ 11.09 (1H, s), 7.74 (1H, d, J = 7.8 Hz), 7.68 (2H, d, J = 7.8 Hz), 7.61 (1H, d, J = 7.8 Hz), 7.35 (2H, dt, J = 1.5, 7.8 Hz), 7.28 (2H, dd, J = 1.5, 7.8 Hz), 7.25 (1H, d, J = 7.8 Hz), 7.08 (2H, t, J = 7.8 Hz), 7.00 (1H, t, J = 7.8 Hz), 6.91 (1H, d, J = 7.8 Hz), 6.78 (1H, dt, J = 1.2, 7.8 Hz), 2.83 (1H, s), 1.98 (3H, s), 1.80 (3H, s); ^{13}C NMR (151 MHz, $CDCl_3$) δ 156.8, 142.3, 138.5, 131.1, 130.7, 129.7, 129.1, 128.6, 128.5, 127.5, 127.2, 125.6, 125.3, 122.2, 120.7, 117.9, 81.2, 38.0, 36.9, 31.8; IR (film) 3100, 1653, 1506, 1457, 1224, 1153, 1068, 1038, 1003, 981 cm^{-1}; HRMS (ESI) Calcd for $C_{26}H_{21}O_2^-$ ([M-H]$^-$) 365.1536. Found 365.1545.

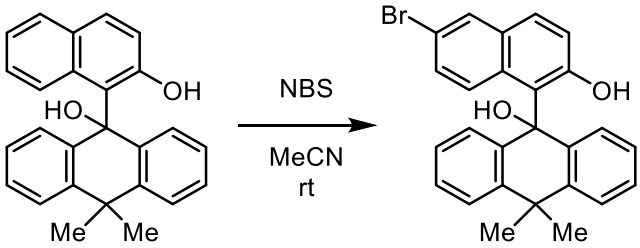

2H-H_2O **2Br**-H_2O

Preparation of 9-(6-bromo-2-hydroxynaphthalen-1-yl)-10,10-dimethyl-9,10-dihydroanthracen-9-ol (2Br-H_2O): To a solution of **2H**-H_2O (109.9 mg, 0.30 mmol) in acetonitrile (MeCN) (3.0 mL) was added *N*-bromosuccinimide (NBS) (53.4 mg, 0.30 mmol). After being stirred at room temperature for 24 h, the resulting mixture was diluted with water and extracted with EA three times. The combined organic extracts were washed with brine, dried over Na_2SO_4, and concentrated under reduced pressure to afford the crude residue. Purification of the residue by column chromatography on silica gel (H/EA = 10:1 as eluent) furnished **2Br**-H_2O in 34% yield (45.4 mg, 0.10 mmol) as a light-purplish solid. **2Br-H_2O:** ^{1}H NMR (600 MHz, $CDCl_3$) δ 11.10 (1H, s), 7.75 (1H, d, J = 2.4 Hz), 7.68 (2H, d, J = 8.1 Hz), 7.65 (1H, d, J = 8.1 Hz), 7.37 (2H, dt, J = 1.5, 8.1 Hz), 7.27 (1H, d, J = 8.1 Hz), 7.25 (2H, d, J = 8.1 Hz), 7.10 (2H, t, J = 8.1 Hz), 6.86 (1H, dd, J = 2.4, 8.1 Hz), 6.79 (1H, d, J = 8.1 Hz), 2.82 (1H, s), 1.96 (3H, s), 1.79 (3H, s); ^{13}C NMR (151 MHz, $CDCl_3$) δ 157.0, 142.3, 138.2, 131.0, 130.3, 129.8, 129.7, 129.3, 128.6, 128.5, 127.6, 127.2, 121.9, 118.3, 116.0, 81.0, 37.9, 36.9, 31.7, one carbon atom was not found probably due to overlapping.; IR (film) 3150, 1617, 1595, 1506, 1486, 1456, 1384, 1228, 1051, 940, 911 cm^{-1}; HRMS (ESI) Calcd for $C_{26}H_{20}BrO_2^-$ ([M-H]$^-$) 443.0641 and 445.0621. Found 443.0648 and 445.0629.

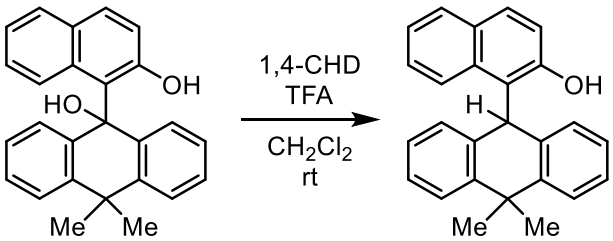

2H-H_2O **2H**-H_2

Preparation of 1-(10,10-dimethyl-9,10-dihydroanthracen-9-yl)-naphthalen-2-ol (2H-H_2): 1,4-CHD (0.40 mL, 5.0 mmol) and trifluoroacetic acid (TFA) (0.23 mL, 2.0 mmol) were added to a solution of **2H**-H_2O (366.5 mg, 1.0 mmol) in CH_2Cl_2 (10.0 mL) at room temperature. After overnight stirring, the reaction mixture was evaporated to afford the crude residue. Purification of the residue was conducted by column chromatography on silica gel (H/EA = 10:1 as eluent) to give a mixture of rotamers of **2H**-H_2 in quantitative yield (350.5 mg, 1.0 mmol) as a yellowish solid. **2H-H_2:** ^{1}H NMR (600 MHz, CD_3CN) *major rotamer* δ 7.81 (1H, d, J = 8.1 Hz), 7.75 (1H, d, J = 8.1 Hz), 7.71 (2H, d, J = 8.1 Hz), 7.46 (1H, s), 7.38 (1H, d, J = 8.1 Hz), 7.22 (2H, t, J = 8.1 Hz), 7.08 (1H, dt, J = 1.8, 8.1 Hz), 6.93 (2H, t, J = 8.1 Hz), 6.91 (1H, d, J = 8.1 Hz), 6.84 (1H, t, J = 8.1 Hz), 6.66 (2H, d, J = 8.1 Hz), 6.37 (1H, s), 2.04 (3H, s), 1.55 (3H, s); ^{13}C NMR (151 MHz, CD_3CN) *major rotamer* δ 154.6, 143.9, 138.4, 132.9, 131.3, 130.1, 129.6, 128.3, 127.5, 126.9, 126.8$_0$, 126.7$_5$, 125.9, 123.5, 122.8, 118.6, 39.2,

39.1, 35.0, 29.6; IR (film) 1653, 1540, 1506, 1472, 1276, 1250, 808 cm^{-1}; HRMS (ESI) Calcd for $C_{26}H_{21}O^-$ ([M-H]$^-$) 349.1587. Found 349.1597.

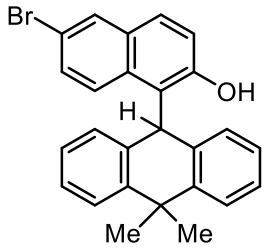

2Br-H$_2$: The title compound was prepared as a yellowish solid from **2Br-**H_2O by following the procedure for **2H**-H_2. ^{1}H NMR (600 MHz, CD_3CN) *major rotamer*δ 7.95 (1H, d, J = 1.8 Hz), 7.76 (1H, d, J = 8.1 Hz), 7.71 (2H, d, J = 8.1 Hz), 7.60 (1H, s), 7.41 (1H, d, J = 8.1 Hz), 7.23 (2H, t, J = 8.1 Hz), 6.94 (2H, t, J = 8.1 Hz), 6.94 (1H, d, J = 8.1 Hz), 6.80 (1H, d, J = 8.1 Hz), 6.63 (2H, d, J = 8.1 Hz), 6.34 (1H, s), 2.02 (3H, s), 1.54 (3H, s); ^{13}C NMR (151 MHz, CD_3CN) *major rotamer*δ 155.1, 143.9, 138.1, 132.6, 131.6, 131.4, 129.4, 128.9, 128.8, 128.3, 127.6, 127.0, 126.8, 123.3, 119.8, 116.6, 39.2, 39.0, 34.8, 29.4; IR (film) 2966, 1700, 1654, 1636, 1540, 1506, 1457, 1360, 1253, 967 cm^{-1}; HRMS (ESI) Calcd for $C_{26}H_{20}BrO^-$ ([M-H]$^-$) 427.0692 and 429.0672. Found 427.0698 and 429.0678.

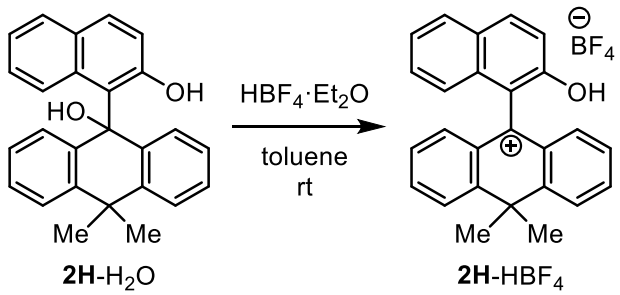

Preparation of 9-(2-hydroxynaphthalen-1-yl)-10,10-dimethyl-9,10-dihydroanthracen-9-ylium tetrafluoroborate (2H-HBF$_4$): **2H-**H_2O (18.3 mg, 0.05 mmol) was treated with tetrafluoroboric acid diethyl ether complex ($HBF_4 \cdot Et_2O$, 8.1 mg, 0.050 mmol) in toluene (1.0 mL) at room temperature for a few minutes to form deep-red precipitation. Precipitation was collected by filtration with toluene and dried under reduced pressure to afford **2H**-HBF_4 in quantitative yield (21.8 mg, 0.050 mmol) as a deep-red solid. **2H-HBF$_4$:** ^{1}H NMR (600 MHz, CD_3CN) δ 8.40 (2H, d, J = 8.1 Hz), 8.35 (2H, t, J = 8.1 Hz), 8.22 (1H, d, J = 8.1 Hz), 8.02 (1H, d, J = 8.1 Hz), 7.94 (2H, d, J = 8.1 Hz), 7.92 (1H, brs), 7.61 (2H, t, J = 8.1 Hz), 7.45 (1H, d, J = 8.1 Hz), 7.44 (1H, t, J = 8.1 Hz), 7.35 (1H, t, J = 8.1 Hz), 6.98 (1H, d, J = 8.1 Hz), 2.03 (3H, s), 1.94 (3H, s); ^{13}C NMR (151 MHz, CD_3CN) δ 197.7, 164.5, 153.0, 147.5, 141.4, 135.0$_1$, 134.9$_7$, 133.5, 131.2, 130.7, 129.5, 129.2, 128.9, 125.7, 125.5, 115.7, 85.0, 46.1, 31.8, 31.2; ^{19}F NMR (376 MHz, CD_3CN) δ –151.7 cm^{-1}; IR (film) 3300, 2950, 1588, 1559, 1484, 1446, 1371, 1349, 1334, 1311, 1265, 1231, 1066, 978, 820 cm^{-1}; HRMS (ESI) Calcd for $C_{26}H_{21}O^+$ ([M-BF$_4$]$^+$) 349.1587. Found 349.1588.

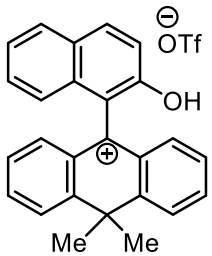

2H-HOTf: The title compound was prepared as a deep-red solid by following the above procedure using trifluoromethanesulfonic acid (HOTf) instead of $HBF_4 \cdot Et_2O$. ^{1}H NMR (600 MHz, CD_3CN) δ 8.39 (2H, d, J = 8.1 Hz), 8.34 (2H, t, J = 8.1 Hz), 8.22 (1H, d, J = 8.1 Hz), 8.12 (1H, br), 8.02 (1H, d, J = 8.1 Hz), 7.95 (2H, d, J = 8.1 Hz), 7.61 (2H, t, J = 8.1 Hz), 7.46 (1H, d, J = 8.1 Hz), 7.44 (1H, t, J = 8.1 Hz), 7.35 (1H, t, J = 8.1 Hz), 6.98 (1H, d, J = 8.1 Hz), 2.03 (3H, s), 1.94 (3H, s); ^{13}C NMR (151 MHz, CD_3CN) δ 197.8, 164.4, 153.1,

147.5, 141.4, 135.0$_2$, 134.9$_6$, 133.5, 131.2, 130.7, 129.5, 129.2, 128.8, 125.7, 125.4, 115.7, 46.0, 31.8, 31.2, one carbon atom was not found probably due to overlapping.; ^{19}F NMR (376 MHz, CD_3CN) δ –79.2, IR (film) 3164, 1590, 1564, 1482, 1448, 1373, 1343, 1284, 1228, 1173, 1028, 982, 818 cm^{-1}; HRMS (ESI) Calcd for $C_{26}H_{21}O^+$ ([M-OTf]$^+$) 349.1587. Found 349.1588.

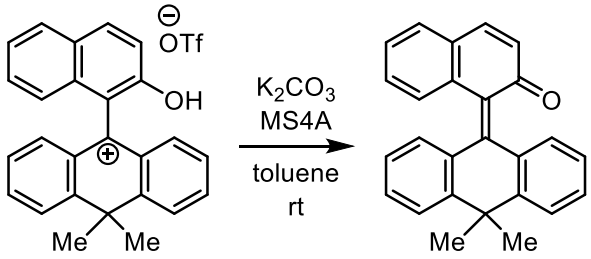

2H-HOTf **2H**

Preparation of 1-(10,10-dimethylanthracen-9(10*H*)-ylidene)-naphthalen-2(1*H*)-one (2H): In a glove box, a suspension of **2H**-HOTf (49.8 mg, 0.10 mmol), 4 Å molecular sieves (MS4A, 200.0 mg), and K_2CO_3 (138.2 mg, 1.0 mmol) in toluene (10.0 mL) was stirred at room temperature overnight. The remaining solid was removed by filtration with toluene and the filtrate was concentrated to afford the crude residue. The resulting residue was dissolved in hexane and filtered for removing KOTf. Concentration of the filtrate furnished analytically pure **2H** in quantitative yield (34.8 mg, 0.10 mmol) as a yellow solid. **2H**: ^{1}H NMR (600 MHz, C_6D_6) δ 7.54 (1H, d, J = 7.8 Hz), 7.32 (1H, d, J = 7.8 Hz), 7.28 (1H, d, J = 7.8 Hz), 7.13 (1H, d, J = 7.8 Hz), 7.08 (1H, d, J = 7.8 Hz), 7.05 (1H, t, J = 7.8 Hz), 7.00 (1H, t, J = 7.8 Hz), 6.96 (1H, t, J = 7.6 Hz), 6.83 (1H, td, J = 1.8, 7.8 Hz), 6.80 (1H, t, J = 7.8 Hz), 6.79 (1H, d, J = 9.6 Hz), 6.67 (1H, t, J = 7.8 Hz), 6.56 (1H, dt, J = 1.8, 7.8 Hz), 6.28 (1H, d, J = 9.6 Hz), 1.64 (6H, s); ^{13}C NMR (151 MHz, C_6D_6) δ 194.8, 149.0, 146.9, 146.2, 141.4, 138.1, 138.0, 135.1, 132.7, 131.0, 129.9, 128.8, 127.6, 126.8, 125.6, 125.3, 124.2, 123.8, 40.8, 28.0; IR (film) 2922, 1659, 1559, 1487, 1465, 1387, 1238, 1203, 830 cm^{-1}; HRMS (ESI) Calcd for $C_{26}H_{21}O^+$ ([M+H]$^+$) 349.1587. Found 349.1585.

Computational Details:

DFT Calculation: The density functional theory (DFT) calculations were carried out using the Gaussian 09 Revision E.01 suite of programs[15] with default thresholds and algorithms unless otherwise noted. All stationary points were verified by the presence of all positive frequencies for local minima or a single negative frequency corresponding to the process of interest for transition states. Reported electronic energies do not include zero-point energy corrections.

Photoexcitation from S_0 to S_1 States: The first excited state of **2H** is reported below. Geometry optimizations were performed using DFT/time-dependent DFT (TD-DFT) with the CAM-B3LYP range-separated exchange correlation functional[16] employing the 6-31+G(d) basis set (CAM-B3LYP/6-31+G(d)). The CH_2Cl_2 solvent effects were taken into account by using the SMD model.[17]

Excited State 1: Singlet-A 3.2802 eV 377.98 nm f=0.2905 <S**2>=0.000

86 -> 93 0.10606 ($2\times(0.10606)^2 = 0.02250$ (2% contribution)

87 -> 93 -0.17186 ($2\times(0.17186)^2 = 0.05907$ (6% contribution)

89 -> 93 -0.11793 ($2\times(0.11793)^2 = 0.02781$ (3% contribution)

90 -> 93 0.12732 ($2\times(0.12732)^2 = 0.03242$ (3% contribution)

92 -> 93 0.63668 ($2\times(0.63668)^2 = 0.81072$ (81% contribution)

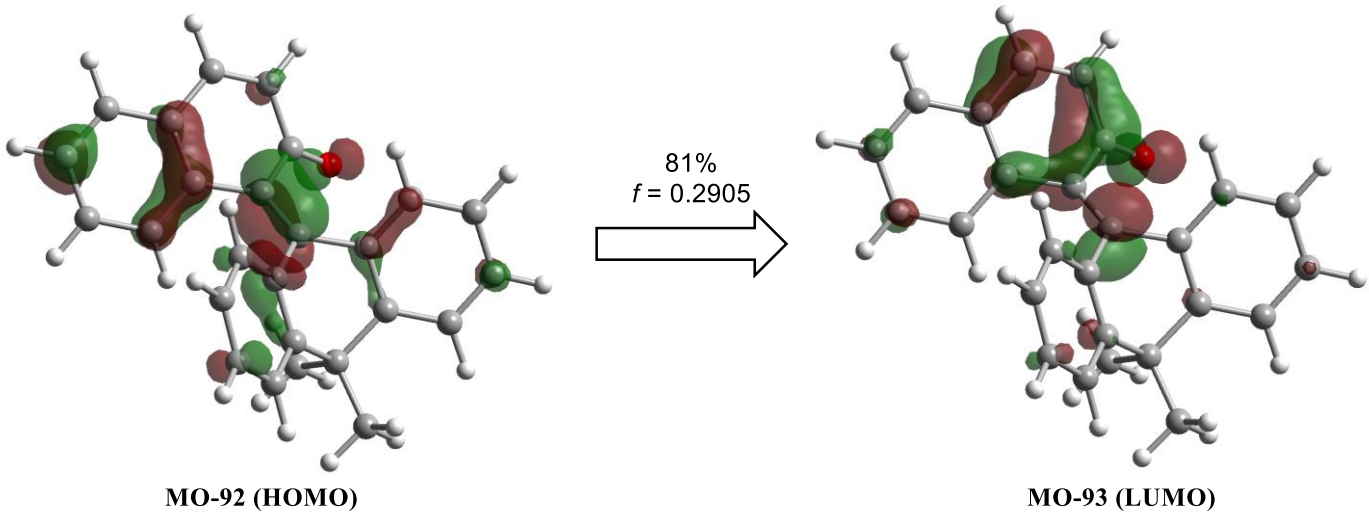

Figure S4. The highest occupied molecular orbital (HOMO) and the lowest unoccupied molecular orbital (LUMO) of **2H** at the geometry optimized in the S_0 state. The contribution (%) of the transition and oscillator strength (*f*) of the excitation is placed over the arrow.

Photoexcitation from $^1S_0$ to $^1S_1$ States: The first excited state of $^1S_0$ geometry of **2H** is reported below. Geometry optimizations in the $^1S_1$ state were performed at the TD-CAMB3LYP/6-31+G(d) level of theory with QC-SCF method.[18] The CH_2Cl_2 solvent effects were taken into account by using the SMD model.

Excited State 1: Singlet-A 0.5826 eV 2128.27 nm f=0.0001 <S**2>=0.000

92 -> 93 0.69367 ($2\times(0.69367)^2 = 0.96236$ (96% contribution)

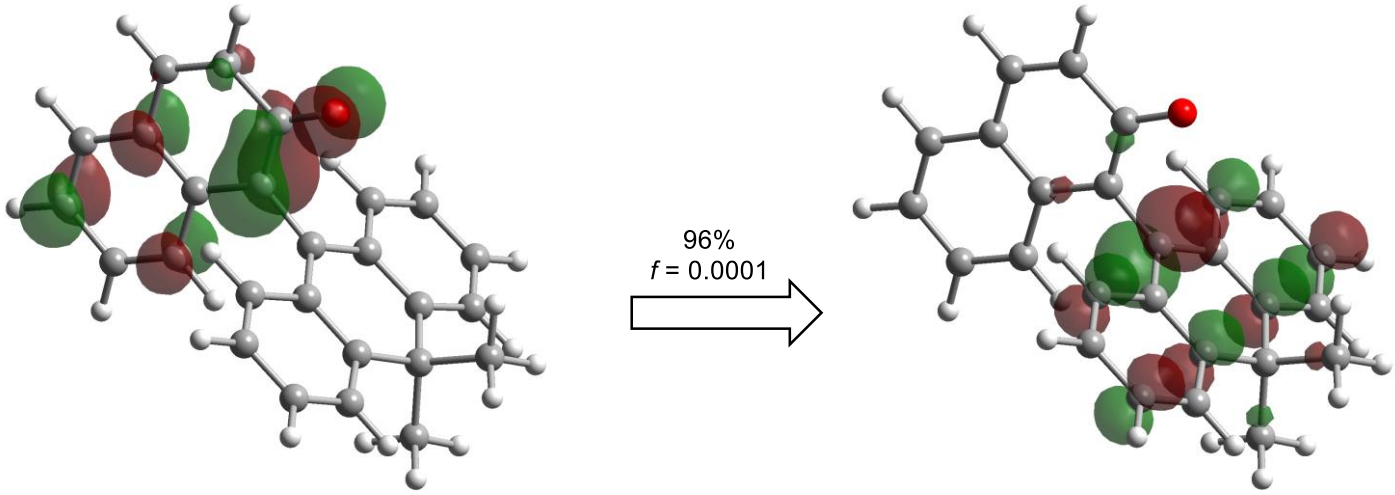

MO-92 (HOMO) **MO-93 (LUMO)**

Figure S5. The highest occupied molecular orbital (HOMO) and the lowest unoccupied molecular orbital (LUMO) of **2H** at the geometry optimized in the $^{t}S_0$ state. The contribution (%) of the transition and oscillator strength (*f*) of the excitation is placed over the arrow.

Estimating Triplet Energy of 2H-H_2: Triplet energy of **2H**-H_2 was estimated through calculation of energy difference between ground-state and excited-state energies at the T_0 geometry of **2H**-H_2. Geometry optimization was performed at the UCAMB3LYP/6-31+G(d) level of theory. The CH_2Cl_2 solvent effects were taken into account by using the SMD model.

$E(S^T_0) = -1078.69522705$ a.u. $E(T_0) = -1078.61546284$ a.u.

$\Delta E(T_0–S^T_0) = 0.07976421$ a.u. = 2.17 eV

Cartesian Coordinates of Calculated Structures

1 *E* = -960.807292395 a.u.

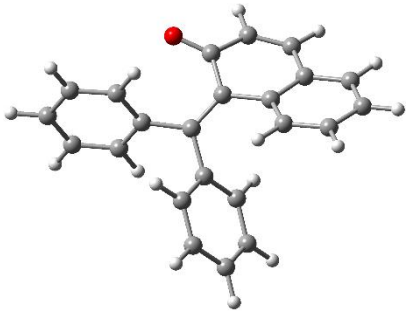

C	-0.429345	-0.927309	0.139863
C	-0.186246	-2.364114	-0.211571
C	-1.269248	-3.021248	-0.957906
C	-2.513672	-2.515601	-0.987566
C	-2.865971	-1.302071	-0.268169
C	-4.208695	-0.936720	-0.112568
C	-4.559096	0.155617	0.667067
C	-3.558447	0.879615	1.317019
C	-2.222407	0.536738	1.151641
C	-1.846364	-0.533901	0.330984
O	0.855705	-2.972768	0.019186
H	-1.021510	-3.970214	-1.424126
H	-3.310668	-3.046750	-1.502955
H	-4.975840	-1.535315	-0.597015
H	-5.602894	0.429785	0.788049
H	-3.820353	1.715115	1.959835
H	-1.462108	1.104294	1.675785
C	0.600914	-0.033316	0.068386
C	0.384992	1.432048	-0.120749
C	-0.420814	1.904438	-1.163022
C	-0.578532	3.270319	-1.373149
C	0.058476	4.185864	-0.537886
C	0.870456	3.725689	0.496871
C	1.045621	2.359426	0.693048
C	2.041583	-0.412855	0.094417
C	2.880429	-0.049753	-0.965400
C	4.241375	-0.336347	-0.922528
C	4.789581	-0.951217	0.201096
C	3.966529	-1.291252	1.273147
C	2.600791	-1.034690	1.214896
H	-0.920448	1.196534	-1.817259
H	-1.200483	3.619458	-2.192579
H	-0.069437	5.252543	-0.698829
H	1.376566	4.432103	1.148794
H	1.690178	2.008481	1.493778
H	2.461856	0.451130	-1.833905
H	4.875390	-0.067551	-1.762740
H	5.854517	-1.162210	0.242646
H	4.387594	-1.767045	2.154398
H	1.960535	-1.314369	2.045111

2H (S_0) *E* = -1077.48159482 a.u.

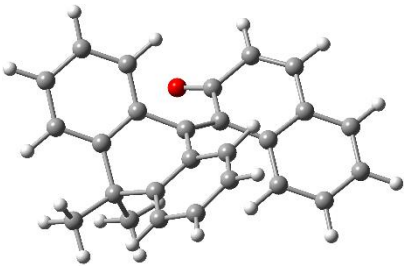

O	0.396758	-3.000105	0.972543
C	-1.540025	1.715873	0.004143
C	-0.406610	1.109223	-0.565721
C	-2.579614	-0.498177	0.231978
C	1.200990	-2.316116	0.350487
C	-3.797176	-1.172634	0.125990
H	-4.692917	-0.754377	0.569997
C	2.306099	-0.074715	0.261794
C	-0.163225	-0.319784	-0.230838
C	-1.550031	-2.267217	-1.074848
H	-0.675601	-2.680954	-1.566765
C	-1.436958	-1.085262	-0.341499
C	1.039024	-0.840630	0.128201
C	2.373973	1.218953	0.787996
H	1.471233	1.708334	1.133816
C	0.379234	1.805711	-1.485774
H	1.221861	1.307983	-1.955069
C	0.086985	3.125890	-1.805392
H	0.700609	3.659461	-2.525537
C	4.725094	-0.023810	-0.019999
H	5.639817	-0.529928	-0.317670
C	-0.997108	3.753758	-1.198959
H	-1.232610	4.787779	-1.435052
C	-3.793220	1.535027	1.161534
H	-4.348812	1.704341	0.233467
H	-3.661153	2.497580	1.663232
H	-4.408661	0.919639	1.823432
C	3.512455	-0.717014	-0.092479
C	4.767707	1.278924	0.458204
H	5.714334	1.807242	0.521934
C	-1.805010	3.050074	-0.308078
H	-2.662357	3.552028	0.125425
C	-1.757839	0.693676	2.297974
H	-2.386180	0.075055	2.947614
H	-1.624398	1.669687	2.777038
H	-0.778823	0.214657	2.223695
C	2.418999	-2.903397	-0.228380
H	2.432750	-3.979306	-0.375395
C	-2.773232	-2.914578	-1.190568
H	-2.848929	-3.833440	-1.764814
C	-2.435902	0.868479	0.917659
C	-3.896086	-2.373975	-0.571250
H	-4.857968	-2.873108	-0.648890
C	3.496959	-2.131982	-0.448803
H	4.422737	-2.569797	-0.814765
C	3.589043	1.888202	0.886724
H	3.613845	2.890972	1.303398

2H ($^1S_0$) *E* = -1077.45494301 a.u.

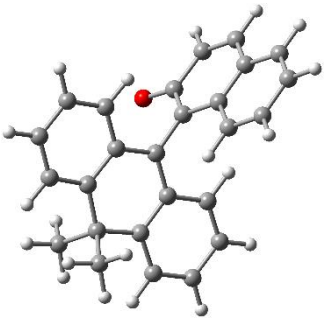

C	1.302184	0.012919	0.689991
C	1.662225	0.024830	2.062434
C	3.090357	0.028100	2.361161
C	4.049267	0.018276	1.402467
C	3.700253	0.006060	0.015138
C	4.658074	-0.006754	-1.008915
C	4.302846	-0.018519	-2.374476
C	2.952755	-0.017645	-2.736669
C	1.980596	-0.006002	-1.764459
C	2.323111	0.005127	-0.333316
O	0.811336	0.032273	3.006780
H	3.361862	0.037358	3.413578
H	5.103190	0.019657	1.669726
H	5.710052	-0.007351	-0.737968
H	5.081486	-0.027668	-3.128700
H	2.667659	-0.025720	-3.783286
H	0.932617	-0.004983	-2.038485
C	-0.115865	0.005056	0.290372
C	-0.828584	1.244730	0.126313
C	-0.135407	2.477056	0.225336
C	-0.784281	3.690840	0.087453
C	-2.153477	3.708426	-0.168149
C	-2.847296	2.503213	-0.281739
C	-2.216812	1.266092	-0.143690
C	-3.044970	-0.010823	-0.285102
C	-2.205435	-1.278907	-0.131530
C	-2.824536	-2.522892	-0.259029
C	-2.120181	-3.720796	-0.132859
C	-0.751689	-3.688519	0.124864
C	-0.113830	-2.467677	0.251497
C	-0.817724	-1.242407	0.139813
C	-3.710724	-0.020308	-1.681324
C	-4.146531	-0.010811	0.799203
H	0.934167	2.454879	0.411099
H	-0.226980	4.618831	0.177369
H	-2.683877	4.649525	-0.278802
H	-3.912924	2.540833	-0.483137
H	-3.889436	-2.572133	-0.461805
H	-2.641950	-4.667575	-0.235853
H	-0.186177	-4.610566	0.224168
H	0.955510	-2.434430	0.437038
H	-4.339183	-0.906226	-1.809326
H	-2.956097	-0.020350	-2.474778
H	-4.347655	0.858370	-1.817371
H	-3.708009	-0.003220	1.802026
H	-4.780757	-0.897872	0.710441
H	-4.790155	0.868476	0.701114

2H-H_2 (S_0) *E* = -1078.71412258 a.u.

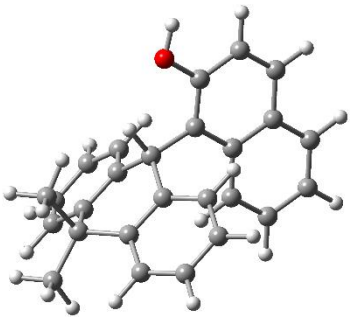

C	3.494146	-0.000009	1.587143
H	4.103910	-0.887938	1.787135
H	2.658391	-0.000063	2.292619
H	4.103787	0.888006	1.787125
C	-1.505799	-0.000047	-1.626252
H	-0.426943	-0.000068	-1.719991
C	0.200768	0.000020	0.871707
H	0.490711	0.000044	1.928322
C	-1.320550	0.000048	0.871549
C	2.713542	2.426094	-0.651557
H	3.745141	2.445448	-0.981752
C	0.821383	-1.262840	0.279859
C	2.168305	1.253076	-0.117770
C	1.963719	3.592498	-0.768927
H	2.417683	4.485912	-1.188966
C	0.081348	-2.442575	0.175444
H	-0.955241	-2.450618	0.495950
C	1.963506	-3.592629	-0.768767
H	2.417406	-4.486088	-1.188778
C	0.081471	2.442598	0.175310
H	-0.955120	2.450721	0.495806
C	0.821434	1.262823	0.279792
C	4.284164	0.000000	-0.762286
H	4.050540	-0.000459	-1.832270
H	4.904644	-0.872511	-0.545188
H	4.904089	0.873072	-0.545829
C	0.640747	-3.605229	-0.342532
H	0.042675	-4.509110	-0.418382
C	2.168257	-1.253181	-0.117714
C	3.022188	-0.510000	0.110416
O	-1.260035	0.000123	3.234793
H	-1.852914	0.000221	4.004777
C	2.713402	-2.426265	-0.651466
H	3.744981	-2.445716	-0.981696
C	0.640951	3.605193	-0.342715
H	0.042936	4.509107	-0.418616
C	-1.990311	0.000105	2.077345
C	-2.098635	0.150000	-0.332721
C	-3.405495	0.000139	2.153399
H	-3.884434	0.000183	3.129710
C	-3.521860	0.000046	-0.261993
C	-2.274127	-0.000080	-2.764241
H	-1.790687	-0.000128	-3.737251
C	-4.291010	0.000011	-1.454782

H	-5.375057	0.000032	-1.370801
C	-4.151074	0.000110	1.009997
H	-5.236488	0.000136	1.062599
C	-3.685317	-0.000052	-2.684835
H	-4.280649	-0.000081	-3.593284

2H-H_2 (T_0) E = -1078.61546284 a.u.

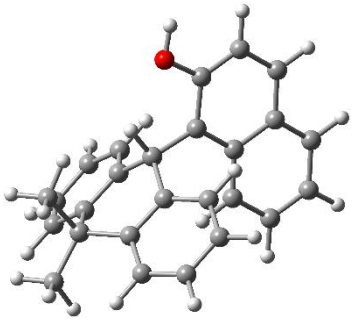

C	3.494362	-0.000114	1.582414
H	4.104264	-0.888060	1.781706
H	2.658973	-0.000362	2.288445
H	4.104025	0.887919	1.782047
C	-1.511405	0.000363	-1.621900
H	-0.433091	0.000379	-1.720131
C	0.196198	-0.000209	0.866100
H	0.483391	-0.000382	1.922950
C	-1.316851	-0.000291	0.851195
C	2.713244	2.428411	-0.650089
H	3.744930	2.448316	-0.979940
C	0.820890	-1.264246	0.275116
C	2.167444	1.253572	-0.120350
C	1.964222	3.595579	-0.763500
H	2.419027	4.490053	-1.180285
C	0.081149	-2.444569	0.174828
H	-0.956231	-2.452448	0.493732
C	1.964620	-3.595223	-0.764772
H	2.419519	-4.489501	-1.181876
C	0.080868	2.444390	0.175696
H	-0.956511	2.452049	0.494607
C	0.820733	1.264109	0.275557
C	4.282021	0.000415	-0.768284
H	4.047015	0.000248	-1.837948
H	4.902757	-0.872094	-0.552078
H	4.902189	0.873371	-0.552233
C	0.641669	-3.608348	-0.338705
H	0.044687	-4.513129	-0.411601
C	2.167602	-1.253413	-0.120797
C	3.021162	0.000103	0.106055
O	-1.226672	-0.001022	3.234067
H	-1.764395	-0.001269	4.046117
C	2.713518	-2.428015	-0.650953
H	3.745198	-2.447713	-0.980821
C	0.641269	3.608412	-0.337425
H	0.044194	4.513158	-0.409992
C	-2.034152	-0.000671	2.142243
C	-2.093959	0.000015	-0.353124
C	-3.387301	-0.000656	2.216824
H	-3.886499	-0.000937	3.182179
C	-3.540357	0.000023	-0.268007
C	-2.297821	0.000706	-2.812486
H	-1.797966	0.000985	-3.776330
C	-4.287088	0.000355	-1.443406
H	-5.371917	0.000361	-1.377690
C	-4.160922	-0.000298	1.012567
H	-5.244734	-0.000293	1.072493
C	-3.660802	0.000695	-2.724322
H	-4.277337	0.000962	-3.618736

2H-Int1 (S_0) E = -1077.46848133 a.u.

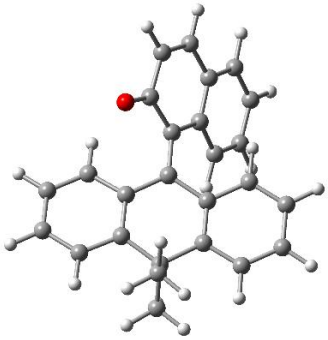

C	-1.209378	0.689706	-0.323877
C	-1.462160	1.759479	-1.301396
C	-2.861349	1.981861	-1.671141
C	-3.884354	1.308419	-1.110194
C	-3.667873	0.336001	-0.067826
C	-4.758281	-0.262318	0.587616
C	-4.565057	-1.128985	1.646280
C	-3.257822	-1.383986	2.085589
C	-2.176185	-0.802897	1.451195
C	-2.341740	0.037365	0.326785
O	-0.574081	2.388027	-1.911471
H	-3.029101	2.733916	-2.436712
H	-4.909038	1.510746	-1.414822
H	-5.763548	-0.016874	0.253714
H	-5.413143	-1.585752	2.147610
H	-3.089656	-2.031973	2.941444
H	-1.178884	-0.995226	1.833000
C	0.127271	0.243296	-0.143338
C	1.177759	1.190636	0.203111
C	0.824893	2.503739	0.592995
C	1.774988	3.435053	0.947646
C	3.122828	3.065370	0.951405
C	3.482172	1.762426	0.649814
C	2.528682	0.798432	0.298205
C	2.986728	-0.634336	0.097002
C	1.838949	-1.582515	-0.208067
C	2.143398	-2.932078	-0.434062
C	1.179640	-3.843351	-0.828475
C	-0.129993	-3.410481	-1.050827
C	-0.451303	-2.089780	-0.826217
C	0.500437	-1.159490	-0.345129
C	3.702376	-1.107955	1.386547
C	3.985413	-0.679696	-1.086769
H	-0.220912	2.777752	0.625726
H	1.476628	4.438896	1.233751
H	3.888655	3.786229	1.223478

H	4.529727	1.487773	0.703896
H	3.165039	-3.276157	-0.316780
H	1.452368	-4.881392	-0.995884
H	-0.886184	-4.099741	-1.413869
H	-1.458386	-1.758118	-1.037748
H	4.049667	-2.138611	1.279597
H	3.028273	-1.061324	2.247765
H	4.575450	-0.487258	1.601754
H	3.503451	-0.363631	-2.017255
H	4.377626	-1.689812	-1.229300
H	4.834377	-0.017154	-0.898826

2H-TS1 (S_0) *E* = -1077.46639587 a.u.

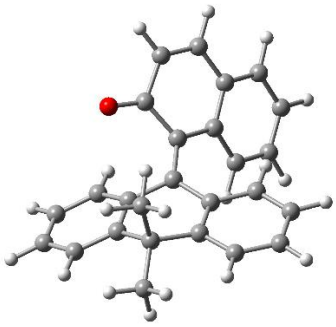

C	-1.147230	-0.662202	0.233534
C	-1.208211	-1.772352	1.221741
C	-2.478600	-1.894049	1.953366
C	-3.594131	-1.227919	1.606929
C	-3.623204	-0.362098	0.448451
C	-4.838467	0.136284	-0.044045
C	-4.885163	0.851012	-1.229289
C	-3.704146	1.052060	-1.952526
C	-2.497328	0.574422	-1.469138
C	-2.414866	-0.099631	-0.234994
O	-0.260968	-2.494716	1.562491
H	-2.469359	-2.594001	2.783741
H	-4.518838	-1.374901	2.160544
H	-5.751166	-0.069765	0.509582
H	-5.831351	1.227355	-1.606536
H	-3.730858	1.574915	-2.904384
H	-1.595107	0.719348	-2.055360
C	0.123048	-0.148988	-0.076855
C	1.184970	-1.088261	-0.434647
C	0.816852	-2.293722	-1.064657
C	1.763852	-3.200143	-1.499110
C	3.114266	-2.905678	-1.317698
C	3.494737	-1.700266	-0.741014
C	2.548442	-0.763818	-0.314343
C	2.961529	0.554839	0.315639
C	1.873628	1.615881	0.126155
C	2.219045	2.967503	0.250245
C	1.268410	3.976418	0.260949
C	-0.081516	3.643060	0.195015
C	-0.447075	2.315363	0.080140
C	0.503863	1.279120	-0.007573
C	4.321066	1.025715	-0.230769
C	3.115036	0.326867	1.844289
H	-0.235525	-2.499236	-1.223269
H	1.457724	-4.123598	-1.981228
H	3.876899	-3.604909	-1.649127
H	4.552527	-1.494078	-0.637222
H	3.258265	3.250124	0.357023
H	1.580374	5.013519	0.344840
H	-0.847478	4.411456	0.241410
H	-1.500051	2.083184	0.057219
H	4.656936	1.934278	0.270839
H	4.282962	1.218407	-1.307940
H	5.093953	0.278738	-0.042388
H	2.176705	-0.013624	2.291972
H	3.417353	1.256404	2.337550
H	3.880945	-0.432399	2.034035

2H-Int2 (S_0) *E* = -1077.47299015 a.u.

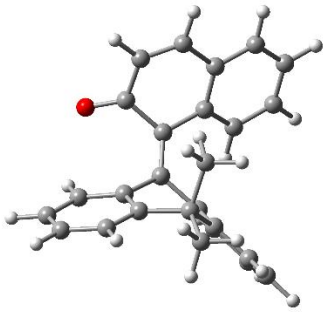

C	0.935106	-0.936276	-0.654821
C	0.854929	-2.420857	-0.455252
C	1.547410	-2.936847	0.731783
C	2.556005	-2.236804	1.274713
C	3.019470	-0.984293	0.690935
C	4.240196	-0.445374	1.105675
C	4.774371	0.674125	0.481224
C	4.087399	1.243476	-0.585967
C	2.857848	0.728933	-0.991761
C	2.276158	-0.363597	-0.344411
O	0.240964	-3.172550	-1.204677
H	1.264593	-3.924979	1.082049
H	3.114788	-2.634987	2.118278
H	4.779206	-0.931638	1.914554
H	5.727690	1.080268	0.805861
H	4.509155	2.091651	-1.117522
H	2.371602	1.172690	-1.845782
C	-0.226975	-0.225866	-0.750418
C	-0.340012	1.259043	-0.686938
C	0.135079	2.103451	-1.689959
C	-0.046035	3.481080	-1.605005
C	-0.715845	4.015635	-0.512128
C	-1.256232	3.169870	0.456303
C	-1.109742	1.786319	0.369012
C	-1.810712	0.804438	1.318245
C	-2.384385	-0.310071	0.425201
C	-3.669145	-0.823642	0.593911
C	-4.187483	-1.776683	-0.282867
C	-3.425809	-2.220912	-1.355495
C	-2.129704	-1.741182	-1.525410
C	-1.593141	-0.816077	-0.629566
C	-2.906237	1.495574	2.137173
C	-0.799698	0.216194	2.331309
H	0.612622	1.679500	-2.566324

H	0.328658	4.126733	-2.393963
H	-0.854993	5.089577	-0.425466
H	-1.822676	3.608492	1.269363
H	-4.295911	-0.470316	1.404367
H	-5.196803	-2.150336	-0.134012
H	-3.832098	-2.939730	-2.061302
H	-1.531111	-2.081578	-2.359507
H	-3.383194	0.783052	2.815455
H	-3.680847	1.942941	1.506298
H	-2.475639	2.281666	2.763220
H	0.035428	-0.293306	1.847864
H	-1.303442	-0.504620	2.984319
H	-0.391657	1.017363	2.956766

2H-TS2 (S_0) *E* = -1077.46760971 a.u.

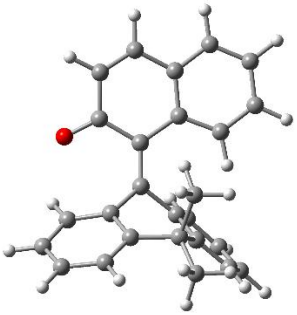

C	1.051738	-0.909440	-0.360289
C	1.267728	-2.393339	-0.396765
C	2.514772	-2.955410	0.109714
C	3.569234	-2.170942	0.362532
C	3.482704	-0.726293	0.290868
C	4.631769	0.003651	0.625588
C	4.610072	1.384114	0.707225
C	3.400689	2.035154	0.482849
C	2.259080	1.321225	0.140574
C	2.257116	-0.077202	-0.017803
O	0.461835	-3.162397	-0.924131
H	2.567230	-4.038386	0.157931
H	4.525207	-2.602163	0.649366
H	5.544743	-0.545123	0.841781
H	5.506533	1.940577	0.963579
H	3.333455	3.115254	0.577106
H	1.359117	1.893688	0.003013
C	-0.220332	-0.409341	-0.541123
C	-0.514443	1.023046	-0.802961
C	-0.034655	1.649970	-1.954295
C	-0.379428	2.968639	-2.225173
C	-1.199624	3.658871	-1.336601
C	-1.707372	3.020165	-0.205681
C	-1.395275	1.687803	0.062430
C	-1.986799	0.873223	1.216302
C	-2.398497	-0.470011	0.586659
C	-3.632550	-1.056264	0.861054
C	-4.068466	-2.187860	0.174188
C	-3.273592	-2.732309	-0.823759
C	-2.015534	-2.193043	-1.078483
C	-1.538073	-1.102365	-0.347468
C	-3.171282	1.596660	1.864895
C	-0.930366	0.655615	2.325575
H	0.619022	1.102815	-2.627585
H	-0.006561	3.455041	-3.121772
H	-1.466786	4.693429	-1.532818
H	-2.371489	3.570002	0.451542
H	-4.290559	-0.612109	1.598282
H	-5.042444	-2.613466	0.399310
H	-3.620660	-3.580022	-1.407558
H	-1.403615	-2.618507	-1.857151
H	-3.569697	1.013540	2.699391
H	-3.984796	1.787260	1.157853
H	-2.845850	2.555313	2.278830
H	-0.032824	0.152684	1.961551
H	-1.356343	0.044656	3.128551
H	-0.630049	1.618806	2.751537

Crystallographic Structure Determination of 1: The single crystal, obtained by the procedure described below, was mounted on MicroMesh. Data of X-ray diffraction were collected at 123 K on a Rigaku FR-X with Pilatus 200K with fine-focus sealed tube Mo/Kα radiation (λ = 0.71075 Å). An absorption correction was made using Crystal Structure. The structure was solved by direct methods and Fourier syntheses, and refined by full-matrix least squares on F^2 by using SHELXL-2014.[19] All non-hydrogen atoms were refined with anisotropic displacement parameters. Hydrogen atoms were placed in calculated positions and their isotropic thermal parameters were refined.
Recrystallization of 1: Recrystallization of **1** was performed by using a CH_2Cl_2/H solvent system at room temperature.

Crystallographic Structure Determination of 2H: The single crystal, obtained by the procedure described below, was mounted on MicroMesh. Data of X-ray diffraction were collected at 123 K on a Rigaku FR-X with Pilatus 200K with fine-focus sealed tube Mo/Kα radiation (λ = 0.71075 Å). An absorption correction was made using Crystal Structure. The structure was solved by direct methods and Fourier syntheses, and refined by full-matrix least squares on F^2 by using SHELXL-2014. All non-hydrogen atoms were refined with anisotropic displacement parameters. Hydrogen atoms were placed in calculated positions and their isotropic thermal parameters were refined.
Recrystallization of 2H: Recrystallization of **2H** was performed by using a Et_2O/H solvent system at room temperature in a glove box.

Crystallographic Structure Determination of 2H-HBF$_4$: The single crystal, which was obtained by the procedure described below, was mounted on MicroMesh. Data of X-ray diffraction were collected at 123 K on a Rigaku MicroMax-007HF with R-AXIS RAPID II with fine-focus sealed tube Cu/Kα radiation (λ = 1.54187 Å). An absorption correction was made using RAPID-AUTO. The structure was solved by direct methods and Fourier syntheses, and refined by full-matrix least squares on F^2 by using SHELXL-2014. All non-hydrogen atoms were refined with anisotropic displacement parameters. A hydrogen atom bonded to the oxygen atom was located from a difference synthesis and its coordinates and isotropic thermal parameters were refined. The other hydrogen atoms were placed in calculated positions and isotropic thermal parameters were refined.
Recrystallization of 2H-HBF$_4$: Recrystallization of **2H-**HBF_4 was performed by using a CH_2Cl_2/H solvent system at room temperature.

Crystallographic Structure Determination of 2H-H$_2$O: The single crystal, obtained by the procedure described below, was mounted on MicroMesh. Data of X-ray diffraction were collected at 123 K on a Rigaku FR-X with Pilatus 200K with fine-focus sealed tube Mo/Kα radiation (λ =

0.71075 Å). An absorption correction was made using Crystal Structure. The structure was solved by direct methods and Fourier syntheses, and refined by full-matrix least squares on F^2 by using SHELXL-2014. All non-hydrogen atoms were refined with anisotropic displacement parameters. A hydrogen atom bonded to the oxygen atom was located from a difference synthesis and its coordinates and isotropic thermal parameters were refined. The other hydrogen atoms were placed in calculated positions and isotropic thermal parameters were refined.

Recrystallization of 2H-H_2O: Recrystallization of **2H-**H_2O was performed by using a CH_2Cl_2/H solvent system at room temperature.

Crystallographic Structure Determination of 2H-H_2: The single crystal, obtained by the procedure described below, was mounted on MicroMesh. Data of X-ray diffraction were collected at 123 K on a Rigaku FR-X with Pilatus 200K with fine-focus sealed tube Mo/Kα radiation (λ = 0.71075 Å). An absorption correction was made using Crystal Structure. The structure was solved by direct methods and Fourier syntheses, and refined by full-matrix least squares on F^2 by using SHELXL-2014. All non-hydrogen atoms were refined with anisotropic displacement parameters. A hydrogen atom bonded to the oxygen atom was located from a difference synthesis and its coordinates and isotropic thermal parameters were refined. The other hydrogen atoms were placed in calculated positions and isotropic thermal parameters were refined.

Recrystallization of 2H-H_2: Recrystallization of **2H-**H_2 was performed by using a CH_2Cl_2/H solvent system at room temperature.

Table S1. Crystal data and structure refinement for quinone methide **1** (CCDC-1993085).

Empirical formula	C26 H20 O1
Formula weight	348.42
Temperature	123(2) K
Wavelength	0.71075 Å
Crystal system	monoclinic
Space group	P 21/c
Unit cell dimensions	a = 10.294(3) Å α = 90°
	b = 16.632(4) Å β = 112.274(2)°
	c = 11.319(3) Å γ = 90°
Volume	1793.3(8) $Å^3$
Z	4
Density (calculated)	1.290 Mg/m^3
Absorption coefficient	0.079 mm^{-1}
F(000)	648
Crystal size	0.10 x 0.070 x 0.060 mm^3
Theta range for data collection	3.0 to 27.5°
Index ranges	–11<=h<=9, –12<=k<=12, –14<=l<=20
Reflections collected	11456
Independent reflections	2875 [R_{int} = 0.0248]
Completeness to theta = 25.242°	98.7%
Absorption correction	Semi-empirical from equivalents
Max. and min. transmission	0.948 and 1.000
Refinement method	Full-matrix least-squares on F^2
Data / restraints / parameters	2875 / 0 / 217
Goodness-of-fit on F^2	1.074
Final R indices [I>2sigma(I)]	R_1 = 0.0354, wR_2 = 0.0765
R indices (all data)	R_1 = 0.0487, wR_2 = 0.0836
Largest diff. peak and hole	0.170 and –0.174 e.$Å^{-3}$

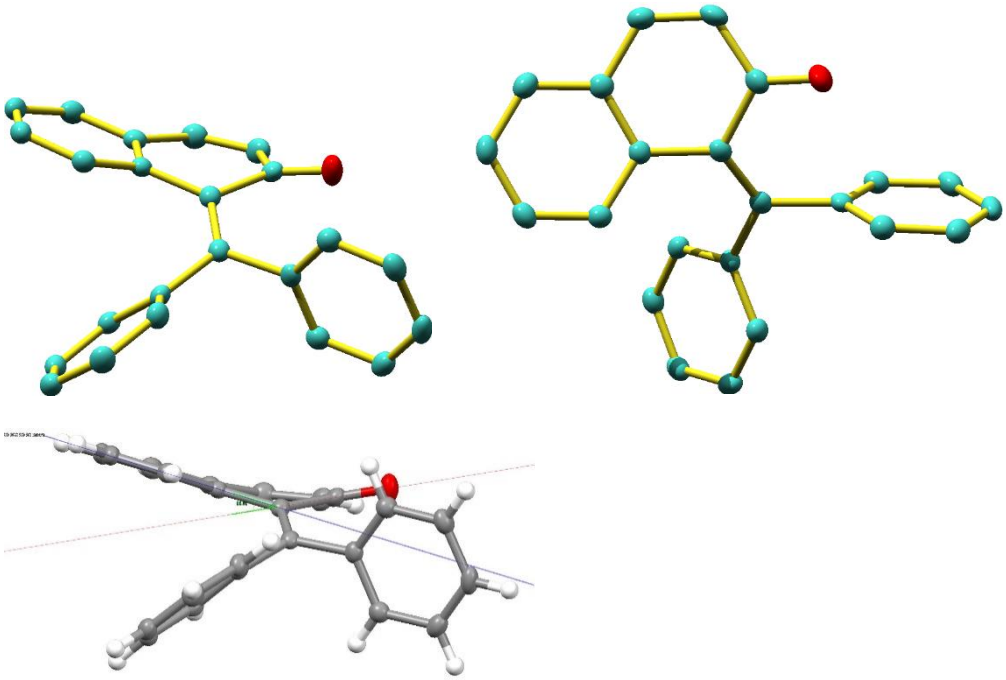

Figure S6. Molecular structure of **1**. Calculated hydrogen atoms are omitted for clarity. The thermal ellipsoids of non-hydrogen atoms are shown at the 50% probability level. Red = oxygen, green = carbon.

Table S2. Crystal data and structure refinement for quinone methide **2H** (CCDC-1993086).

Empirical formula	C23 H16 O1
Formula weight	308.38
Temperature	123(2) K
Wavelength	0.71075 Å
Crystal system	orthorhombic
Space group	P 21/n
Unit cell dimensions	a = 9.3347(13) Å α = 90°
	b = 10.0778(14) Å β = 101.582(3)°
	c = 16.957(3) Å γ = 90°
Volume	1562.7(4) $Å^3$
Z	4
Density (calculated)	1.311 Mg/m^3
Absorption coefficient	0.077 mm^{-1}
F(000)	736
Crystal size	0.500 x 0.260 x 0200 mm^3
Theta range for data collection	3.1 to 27.5°
Index ranges	–12<=h<=12, –20<=k<=20, –13<=l<=13
Reflections collected	30752
Independent reflections	3334 [R_{int} = 0.0141]
Completeness to theta = 25.242°	99.8%
Absorption correction	Semi-empirical from equivalents
Max. and min. transmission	0.938 and 1.000
Refinement method	Full-matrix least-squares on F^2
Data / restraints / parameters	3334 / 0 / 246
Goodness-of-fit on F^2	1.040
Final R indices [I>2sigma(I)]	R_1 = 0.0332, wR_2 = 0.0833
R indices (all data)	R_1 = 0.0448, wR_2 = 0.0849
Largest diff. peak and hole	0.255 and –0.170 e.$Å^{-3}$

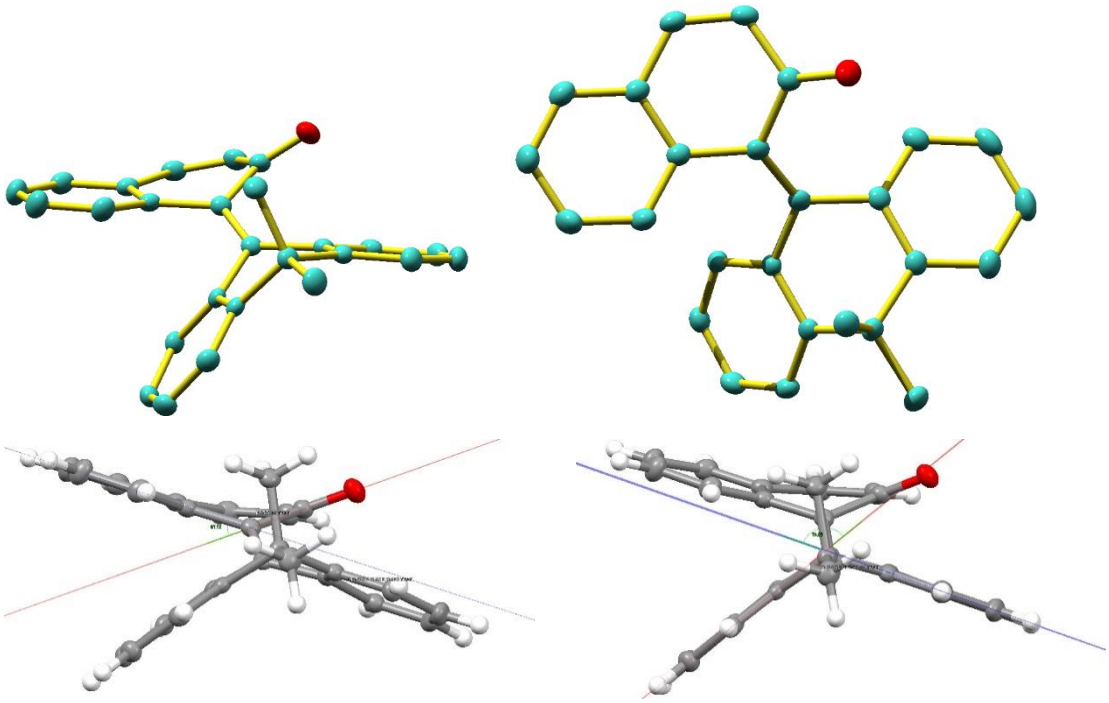

Figure S97 Molecular structure of **2H**. Calculated hydrogen atoms are omitted for clarity. The thermal ellipsoids of non-hydrogen atoms are shown at the 50% probability level. Red = oxygen, green = carbon.

Table S3. Crystal data and structure refinement for **2H**-HBF_4 (CCDC-1993087).

Empirical formula	C26 H21 B1 F4 O1
Formula weight	436.26
Temperature	123(2) K
Wavelength	1.54187 Å
Crystal system	monoclinic
Space group	P 21/n
Unit cell dimensions	a = 7.49820(10) Å α = 90°
	b = 19.0172(4) Å β = 99.675(7)°
	c = 14.6488(3) Å γ = 90°
Volume	2059.13(8) $Å^3$
Z	4
Density (calculated)	1.407 Mg/m^3
Absorption coefficient	0.911 mm^{-1}
F(000)	904
Crystal size	0.10 x 0.050 x 0.050 mm^3
Theta range for data collection	3.844 to 68.165°
Index ranges	–9<=h<=8, –22<=k<=22, –17<=l<=17
Reflections collected	22984
Independent reflections	3738 [R_{int} = 0.0513]
Completeness to theta = 67.687°	99.7%
Absorption correction	Semi-empirical from equivalents
Max. and min. transmission	0.7492 and 1.000
Refinement method	Full-matrix least-squares on F^2
Data / restraints / parameters	3738 / 0 / 292
Goodness-of-fit on F^2	1.054
Final R indices [I>2sigma(I)]	R_1 = 0.0408, wR_2 = 0.1024
R indices (all data)	R_1 = 0.0589, wR_2 = 0.1100
Largest diff. peak and hole	0.169 and –0.243 e.$Å^{-3}$

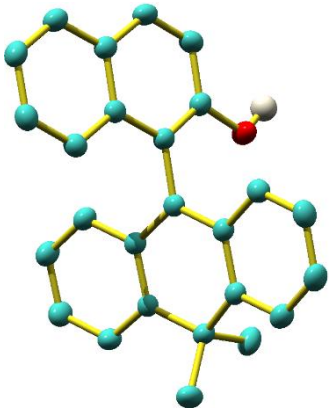

Figure S8. Molecular structure of **2H-**HBF_4. Calculated hydrogen atoms and BF_4^- are omitted for clarity. The thermal ellipsoids of non-hydrogen atoms are shown at the 50% probability level. Red = oxygen, green = carbon.

Table S4. Crystal data and structure refinement for **2H**-H_2O (CCDC-1993087).

Empirical formula	C26 H22 O2
Formula weight	366.44
Temperature	123(2) K
Wavelength	0.71075 Å
Crystal system	monoclinic
Space group	P 21/c
Unit cell dimensions	a = 16.416(3) Å α = 90°
	b = 9.1943(15) Å β = 102.802(4)°
	c = 26.521(5) Å γ = 90°
Volume	3903.4(12) $Å^3$
Z	8
Density (calculated)	1.247 Mg/m^3
Absorption coefficient	0.077 mm^{-1}
F(000)	1552.0
Crystal size	0.100 x 0.090 x 0.070 mm^3
Theta range for data collection	3.126 to 25.499°
Index ranges	–19<=h<=19, –11<=k<=11, –32<=l<=30
Reflections collected	28432
Independent reflections	7232 [R_{int} = 0.1253]
Completeness to theta = 25.499°	99.6%
Absorption correction	Semi-empirical from equivalents
Max. and min. transmission	0.567 and 1.000
Refinement method	Full-matrix least-squares on F^2
Data / restraints / parameters	7232 / 0 / 525
Goodness-of-fit on F^2	1.185
Final R indices [I>2sigma(I)]	R_1 = 0.0781, wR_2 = 0.1704
R indices (all data)	R_1 = 0.1390, wR_2 = 0.2169
Largest diff. peak and hole	0.902 and –0.313 e.$Å^{-3}$

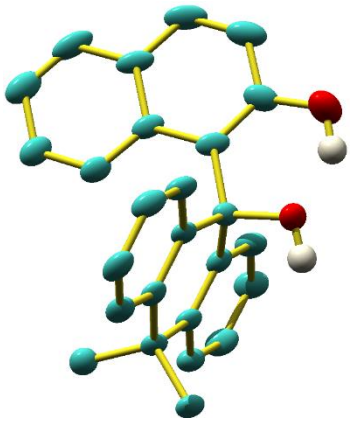

Figure S9. Molecular structure of **2H-**H_2O. Calculated hydrogen atoms are omitted for clarity. The thermal ellipsoids of non-hydrogen atoms are shown at the 50% probability level. Red = oxygen, green = carbon.

Table S5. Crystal data and structure refinement for **2H**-H_2 (CCDC-1993087).

Empirical formula	C26 H22 O
Formula weight	350.44
Temperature	123(2) K
Wavelength	0.71075 Å
Crystal system	orthorhombic
Space group	P 21 21 21
Unit cell dimensions	a = 9.1550(16) Å α = 90°
	b = 12.816(2) Å β = 90°
	c = 15.861(3) Å γ = 90°
Volume	1861.0(6) $Å^3$
Z	4
Density (calculated)	1.251 Mg/m^3
Absorption coefficient	0.074 mm^{-1}
F(000)	744.0
Crystal size	0.260 x 0.030 x 0.020 mm^3
Theta range for data collection	3.021 to 25.495°
Index ranges	–11<=h<=9, –11<=k<=15, –19<=l<=19
Reflections collected	14028
Independent reflections	3444 [R_{int} = 0.0595]
Completeness to theta = 25.242°	99.6%
Absorption correction	Semi-empirical from equivalents
Max. and min. transmission	0.799 and 1.000
Refinement method	Full-matrix least-squares on F^2
Data / restraints / parameters	3444 / 0 / 254
Goodness-of-fit on F^2	1.060
Final R indices [I>2sigma(I)]	R_1 = 0.0473, wR_2 = 0.0851
R indices (all data)	R_1 = 0.0765, wR_2 = 0.0955
Largest diff. peak and hole	0.160 and –0.168 e.$Å^{-3}$

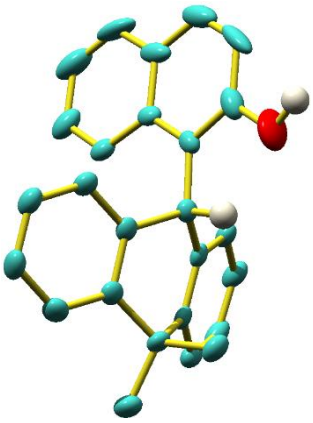

Figure S10. Molecular structure of **2H-**H_2. Calculated hydrogen atoms except for them connected to C9 of the dihydroanthracene subunit are omitted for clarity. The thermal ellipsoids of non-hydrogen atoms are shown at the 50% probability level. Red = oxygen, green = carbon.

References

(1) (a) Horn, M.; Mayr, H. *J. Phys. Org. Chem.* **2012**, *25*, 979–988. (b) Naredla, R. R.; Klumpp, D. A. *Chem. Rev.* **2013**, *113*, 6905−6948.

(2) Wuts, P. G. M. *Greene's Protective Groups in Organic Synthesis*, John Wiley & Sons: Hoboken, 2014.

(3) Naidu, V. R.; Ni, S.; Franzén, J. *ChemCatChem* **2015**, *7*,1896–1905.

(4) Bahr, S. R.; Boudjouk, P. *J. Org. Chem.* **1992**, *57*, 5545–5547.

(5) (a) Wendlandt, A. E.; Stahl, S. S. *Angew. Chem. Int. Ed.* **2015**, *54*, 14638–14658. (b) Tian, J.-J.; Zeng, N.-N.; Liu, N.; Tu, X.-S.; Wang, X.-C. *ACS Catal.* **2019**, *9*, 295–300.

(6) Kumagai, N.; Shibasaki, M. *Angew. Chem. Int. Ed.* **2011**, *50*, 4760–4772.

(7) (a) Jung, M. E.; Speltz, L. M. *J. Am. Chem. Soc.* **1976**, *98*, 7882–7884. (b) Gil-Negrete, J. M.; Sestelo, J. P.; Sarandeses, L. A. *J. Org. Chem.* **2019**, *84*, 9778–9785. (c) Chen, W.; Xie, Z.; Zheng, H.; Lou, H.; Liu, L. *Org. Lett.* **2014**, *16*, 5988–5991. (d) Jung, M. E. *J. Org. Chem.* **1976**, *41*, 1479–1480. (e) Jung, M. E.; Brown, R. W. *Tetrahedron Lett.* **1978**, *31*, 2771–2774. (f) Jung, M. E.; Pan, Y.-G.; Rathke, M. W.; Sullivan, D. F.; Woodbury, R. P. *J. Org. Chem.* **1977**, *42*, 3961–3963. (g) Wan, M.; Meng, Z.; Lou, H.; Liu, L. *Angew. Chem. Int. Ed.* **2014**, *53*, 13845–13849. (h) Liu, X.; Meng, Z.; Li, C.; Lou, H.; Liu, L. *Angew. Chem. Int. Ed.* **2015**, *54*, 6012–6015. (i) Katsina, T.; Clavier, L.; Giffard, J.-F.; Portela da Silva, N. M.; Fournier, J.; Tamion, R.; Copin, C.; Arseniyadis, S.; Jean, A. *Org. Process Res. Dev.* **2020**, *24*, 856–860.

(8) (a) Sugimoto, H.; Nakamura, S.; Ohwada, T. *Adv. Synth. Catal.* **2007**, *349*, 669–679. (b) Pathak, T. P.; Sigman, M. S. *J. Org. Chem.* **2011**, *76*, 9210–9215. (c) Toteva, M. M.; Richard, J. P. In *Advances in Physical Organic Chemistry*, Ed. Richard, J. P. vol 45, 39–91, 2011 Elsevier. (d) Škalamera, Đ.; Mlinarić-Majerski, K.; Kleiner, I. M.; Kralj, M.; Oake, J.; Wan, P.; Bohne, C.; Basarić, N. *J. Org. Chem.* **2017**, *82*, 6006–6021.

(9) (a) Chen, R.; Liu, Y.; Cui, S. *Chem. Commun.* **2018**, *54*, 11753–11756. (b) Chu, M.-M.; Qi, S.-S.; Ju, W.-Z.; Wang, Y.-F.; Chen, X.-Y.; Xu, D.-Q.; Xu, Z.-Y. *Org. Chem. Front.* **2019**, *6*, 1140–1145 and references therein.

(10)(a) Agranat, I.; Tapuhi, Y. *J. Am. Chem. Soc.* **1978**, *100*, 5604–5609. (b) Feringa, B. L.; Jager, W. F.; de Lange, B. *J. Chem. Soc., Chem. Commun.* **1993**, 288–290.

(11)Lewis, T. W.; Duesler, E. N.; Kress, R. B.; Curtin, D. Y.; Paul, I. C. *J. Am. Chem. Soc.* **1980**, *102*, 4659–4664.

(12)(a) Chikashita, H.; Miyazaki, M.; Itoh, K. *Synthesis* **1984**, 308–310. (b) Chikashita, H.; Miyazaki, M.; Itoh, K. *J. Chem. Soc., Perkin Trans. 1* **1987**, 699–706. (c) Zhu, C.; Saito, K.; Yamanaka, M.; Akiyama, T. *Acc. Chem. Res.* **2015**, *48*, 388–398.

(13)(a) Yanai, T.; Tew, D. P.; Handy, N. C. *Chem. Phys. Lett.* **2004**, *393*, 51–57. (b) Gaussian 09, Revision D.01. Frisch, M. J. et al. Gaussian, Inc.: Wallingford, CT, 2009. (c) Marenich, A. V.;

Cramer, C. J.; Truhlar, D. G. *J. Phys. Chem. B* **2009**, *113*, 6378–6396.

(14) Nishiuchi, T.; Ito, R.; Stratmann, E.; Kubo, T. *J. Org. Chem* **2020**, *85*, 179–186.

(15) Gaussian 09, Revision E.01, Frisch, M. J.; Trucks, G. W.; Schlegel, H. B.; Scuseria, G. E.; Robb, M. A.; Cheeseman, J. R.; Scalmani, G.; Barone, V.; Mennucci, G. B.; Petersson, A.; Nakatsuji, H.; Caricato, M.; Li, X.; Hratchian, H. P.; Izmaylov, A. F.; Bloino, J.; Zheng, G.; Sonnenberg, J. L.; Hada, M.; Ehara, M.; Toyota, K.; Fukuda, R.; Hasegawa, J.; Ishida, M.; Nakajima, T.; Honda, Y.; Kitao, O.; Nakai, H.; Vreven, T.; Montgomery, Jr., J. A.; Peralta, J. E.; Ogliaro, F.; Bearpark, M.; Heyd, J. J.; Brothers, E.; Kudin, K. N.; Staroverov, V. N.; Keith, T.; Kobayashi, R.; Normand, J.; Raghavachari, K.; Rendell, A.; Burant, J. C.; Iyengar, S. S.; Tomasi, J.; Cossi, M.; Rega, N.; Millam, J. M.; Klene, M.; Knox, J. E.; Cross, J. B.; Bakken, V.; Adamo, C.; Jaramillo, J.; Gomperts, R.; Stratmann, R. E.; Yazyev, O.; Austin, A. J.; Cammi, R.; Pomelli, C.; Ochterski, J. W.; Martin, R. L.; Morokuma, K.; Zakrzewski, V. G.; Voth, G. A.; Salvador, P.; Dannenberg, J. J.; Dapprich, S.; Daniels, A. D.; Farkas, Ö.; Foresman, J. B.; Ortiz, J. V.; Cioslowski, J.; Fox, D. J. Gaussian, Inc., Wallingford CT, 2013.

(16) Yanai, T.; Tew, D. P.; Handy, N. C. Chem. Phys. Lett. 2004, 393, 51−57.

(17) Marenich, A. V.; Cramer, C. J.; Truhlar, D. G. J. Phys. Chem. B 2009, 113, 6378−6396.

(18) Bacskay, G. B. Chem. Phys. 1981, 61, 385–404.

(19) Sheldrick, G. M. Acta Cryst. 2015, C71, 3−8.

Chapter 3

Dehydridative Oxidation of Benzylic Alcohols under Aerobic Photoirradiation Conditions

Abstract

An o-quinone methide (o-QM) featuring an overcrowded olefinic framework is introduced, which exhibits dehydridation activity owing to its enhanced zwitterionic character, particularly through photoexcitation. An experimental analysis and density functional theory calculations provide mechanistic insights; the ground-state zwitterionic intermediate abstracts a hydride and proton simultaneously, and the active oxygen species facilitate catalyst regeneration.

Introduction

An *o*-quinone methide (*o*-QM) was developed to serve as a catalyst for the dehydridative oxidation of benzylic alcohols. The introduction of an overcrowded olefinic component into the *o*-QM distorted its structure and was found to be effective in imparting triarylmethylium character and regenerability. The zwitterionc resonance form of the *o*-QM generated by photoexcitation and subsequent relaxation exhibited the dehydridation activity. Density functional theory calculations were performed to elucidate the operative catalytic process.

Results and Discussion

We theoretically and experimentally verified that the zwitterionic resonance form of *o*-QM **2H** can be effectively produced under visible-light irradiation, and aimed to apply **2H** as a dehydridation catalyst. Therefore, we chose the dehydridative oxidation of secondary benzylic alcohols as a model reaction to evaluate the intrinsic reactivity of **2H**. Since the simple treatment of 1-(4-methylphenyl)ethanol (**3a**) with 5 mol% of **2H** in dichloromethane at ambient temperature for 12 h produced no corresponding ketone, we first verified the effect of the Brønsted acid co-catalyst using MsOH (5 mol%), which gave 4-methyl acetophenone (**4a**) was obtained in 4% yield (entry 1). On the other hand, when the reaction was carried out under similar conditions but under blue LED irradiation (456 nm), **4a** was obtained in 17% yield, which was larger than the amount of **2H** used as catalyst (entry 2), suggesting that **2H** functions as a dehydridation catalyst (turnover number = >3). Subsequent experiments to investigate the regeneration process of **2H** revealed that a small amount of oxygen could oxidize **2H**-H_2 under photo irradiation, and the catalytic efficiency is greatly enhanced when the reaction is conducted under air or oxygen atmosphere, while the oxidation was suppressed under argon atmosphere (entries 3-5). Furthermore, hydrogen peroxide was detected s a Ti-oxo-complex in the crude reaction mixture, confirming the role of oxygen as a terminal oxidant.[1] This observation suggested that the regeneration process of **2H** was likely facilitated by active oxygen species, such as singlet oxygen or superoxide.[2] In the UV-vis spectrum of **2H**-H_2, the absorption terminus reaches 470 nm, indicating that **2H**-H_2 can be excited by blue-light irradiation, thereby sensitizing O_2 for excitation. The energy of **2H**-H_2 in the excited state was estimated to be 2.17 eV, which is sufficient to activate O_2 in the ground state. Although the TD-DFT analysis also suggested the possibility of another process involving the electron-donor-acceptor (EDA) complex of **2H**-H_2 and O_2 followed by photoexcitation, careful examination of the UV-vis spectra of **2H**-H_2 under both Ar and O_2 atmospheres did not provide any evidence for the formation of the EDA complex. Next, we attempted to oxidize **3a** by employing **2H**-H_2 as a catalyst under aerobic photoirradiation conditions, and observed similar reactivity to that of **2H**, confirming the turnover of the catalyst (entry 6). A further important finding was that a bromo substituent on the 2-naphthol subunit of the catalyst was effective for improving the catalytic activity, and the 6-bromo derivative **2Br**-H_2 promoted an almost

complete conversion of **3a** to **4a** within 12 h (entry 7). The reason for this increased reactivity is not yet to be clarified, but it is probably due to the extended absorption wavelength induced by the introduction of the bromo appendage. Notably, the importance of the overcrowded olefinic component of **2H** to act as a competent dehydridation catalyst was verified by comparing its reactivity to that of **1** (entry 8).

Table 1 Optimization of the Reaction Conditions for Dehydridative Oxidation of Secondary Benzylic Alcohol 3a[a]

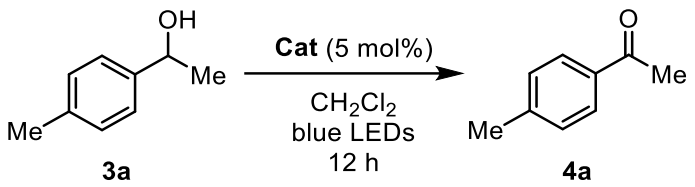

Entry	Catalyst	Yield (%)[b]	note
1	**2H**	4	MsOH (5 mol%) without photoirradiation
2	**2H**	17	under Ar
3	**2H**	51	under air
4	**2H**	59	under O_2
5	**2H**	4	under Ar (degassed)
6	**2H-H$_2$**	76	under O_2
7	**2Br-H$_2$**	97	under O_2
8	**1**	8	under O_2

[a] Reaction was performed with 0.1 mmol of **3a** in the presence of 5 mol% of catalyst in CH_2Cl_2 under blue LEDs irradiation (456 nm) at ambient temperature for 12 h.

[b] ^{1}H NMR yield (400 MHz) determined by trimethylsilylbenzene as the internal standard.

The substrate scope for the oxidation of secondary benzylic alcohols **3** under the dehydridative catalysis of **2Br**-H_2 was explored and the representative results are shown in Table 2. In general, smooth conversion of **3** was achieved using 5 mol% of **2Br-H$_2$** to afford the corresponding ketones **4** in high yield. The introduction of various groups to the aromatic substituent of **3** was allowed regardless of their position and electronic character, but the attachment of an electron-donating group tended to decrease the reactivity (entries 1~10). Variation of the alkyl substituent (R) of **3** was also

possible, both liner and branched chains were well accommodated (entries 11~15). When a diol was used as the substrate, chemoselective oxidation of a benzylic alcohol over an aliphatic alcohol was achieved (entry 16). It should be noted that this protocol is scalable, as demonstrated with **3a** as the substrate (entry 17). However, as expected, the oxidation of aliphatic alcohols was not successful under the present reaction conditions ($Ph(CH_2)_3OH$: <5%, cyclohexanol: 5%), and competitive side reactions were inevitable for allylic and propargylic alcohols, resulting in complex mixtures.

Table 2 Scope of the Catalytic Dehydridative Oxidation of Secondary Benzylic Alcohols **3**[a]

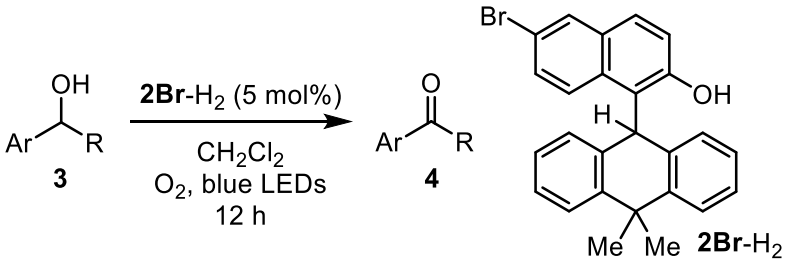

Entry	Ar, R	**3**	Yield (%)[b]	**4**
1	4-$CF_3C_6H_4$, Me	**3b**	85	**4b**
2	4-NCC_6H_4, Me	**3c**	94	**4c**
3	4-ClC_6H_4, Me	**3d**	84	**4d**
4	4-BrC_6H_4, Me	**3e**	97	**4e**
5	C_6H_5, Me	**3f**	90	**4f**
6	3-ClC_6H_4, Me	**3g**	86	**4g**
7	3-MeC_6H_4, Me	**3h**	86	**4h**
8	3-$MeOC_6H_4$, Me	**3i**	95	**4i**
9	2-ClC_6H_4, Me	**3j**	89	**4j**
10	2-MeC_6H_4, Me	**3k**	72	**4k**
11	C_6H_5, Et	**3l**	98	**4l**
12	C_6H_5, ^{n}Pr	**3m**	99	**4m**
13	C_6H_5, ^{i}Bu	**3n**	84	**4n**
14	C_6H_5, ^{i}Pr	**3o**	87	**4o**
15	C_6H_5, ^{c}Hex	**3p**	94	**4p**
16	C_6H_5, $(CH_2)_2OH$	**3q**	77	**4q**
17[c]	4-MeC_6H_4, Me	**3a**	74	**4a**

[a] Unless otherwise noted, reaction was conducted on 0.1 mmol scale with 5 mol% of **2Br**-H_2 in CH_2Cl_2

under photoirradiation (456 nm) for 12 h.

[b] Isolated yield was reported.

[c] 5 mmol scale reaction.

Having established the conditions for the oxidation of secondary benzylic alcohols, we next turned our attention to the oxidation of primary alcohols **5**, the benzylic hydrogens of which are less hydridic. In this case, controlling product distribution between the aldehyde and carboxylic acid is often problematic.[3] However, we expected that aerobic oxidation under photo irradiation using **2Br** catalyst would yield mainly carboxylic acids for the following reasons: 1) hydrogen peroxide is generated in the catalyst-regeneration process, and 2) the aldehyde initially formed would be converted into a perhydrate with an acetal hydrogen, which is more reactive toward dehydridation than the benzylic hydrogen of the starting primary alcohol (Scheme 1).

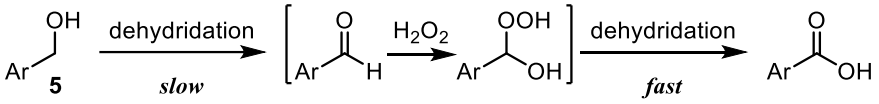

Scheme 1 Dehydridative oxidation of a primary benzylic alcohol to carboxylic acid

As an initial attempt, 1-(4-chlorophenyl)methanol (**5a**) was reacted under optimal reaction conditions optimized for the oxidation of secondary alcohols for 24 h, which gave the corresponding carboxylic acid **6a** albeit in a very low yield, as determined after conversion to methyl ester **7a** (Table 3, entry 1).

Table 3 Dehydridative Oxidation of Primary Benzylic Alcohols 5[a]

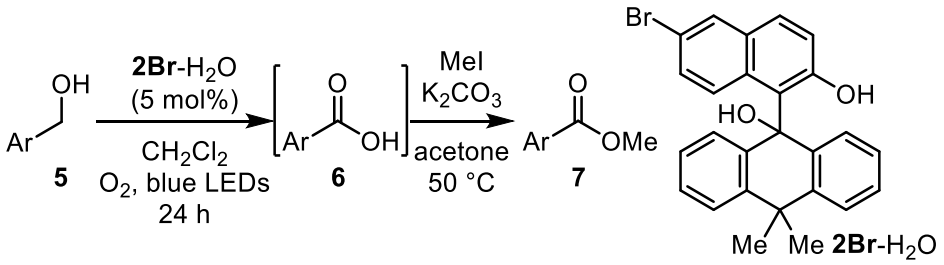

Entry	Ar	**5**	Yield (%)[b]	**7**
1[c]	4-ClC_6H_4	**5a**	11	**7a**
2	4-ClC_6H_4	**5a**	74	**7a**
3	4-$MeOC_6H_4$	**5b**	94	**7b**
4	4-MeC_6H_4	**5c**	63	**7c**
5	4-$^tBuC_6H_4$	**5d**	69	**7d**
6	4-BrC_6H_4	**5e**	86	**7e**

7	4-$CF_3C_6H_4$	**5f**	77	**7f**
8	4-NCC_6H_4	**5g**	81	**7g**
9	4-$O_2NC_6H_4$	**5h**	78	**7h**
10	3-ClC_6H_4	**5i**	64	**7i**
11	2-MeC_6H_4	**5j**	64	**7j**

[a] Unless otherwise noted, reaction was conducted on 0.1 mmol scale with 5 mol% of **2Br**-H_2O in CH_2Cl_2 under photoirradiation (456 nm) for 24 h.

[b] Isolated yield of methyl ester **7** was reported.

[c] **2Br**-H_2 was used as the catalyst.

Interestingly, the use of the hydrated form of **2Br** (**2Br**-H_2O) as a catalyst greatly improved the catalytic efficiency and allowed the isolation of **7a** in 74% yield. It means that the photo-induced generation of catalytically active **2Br** was operative (entry 2).[4] To investigate the experimental support for the dehydridative oxidation of the perhydrate generated from the transiently formed aldehyde, we explored the reaction in the presence of methanol. If the formation of hemiacetal from the aldehyde and methanol competed with the generation of the perhydrate, subsequent dehydridation of the hemiacetal would directly give **7a**. In fact, when 10 equivalents of methanol was added to the reaction of **5a** under otherwise sane conditions to those for entry 1, **7a** was obtained in 35% yield, and at the same time aldehyde **8a** was also produced (23%) (Scheme 2).

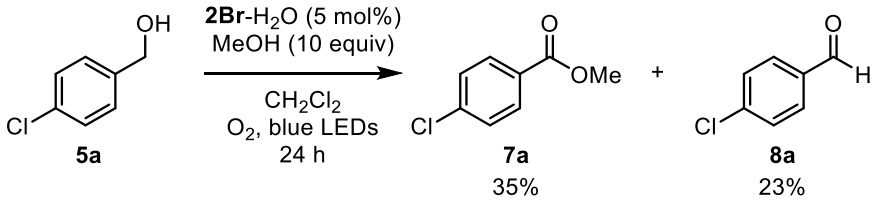

Scheme 2 Trapping experiment of intermediary oxonium ion with methanol

Although this result clearly demonstrated that the oxidation of the presumed perhydrate was mediated, the presence of methanol reduced the reactivity to a non-negligible level. We inferred that methanol might play an important role in inhibiting the hydrogen-bonding interactions between **2Br** and **5a** to promote dehydridative oxidation. The theoretical analysis of the possible transition states of the **2Br**-promoted dehydridation reaction revealed a structure in which the hydrogen bond between the OH proton of the starting benzylic alcohol and the aryloxide moiety of **2Br** contributes to the placement of the benzylic hydrogen close to the carbocationic site of the catalyst, and the concerted deprotonative dehydridation pathway works in favor of obtaining the aldehyde (Figure 1).

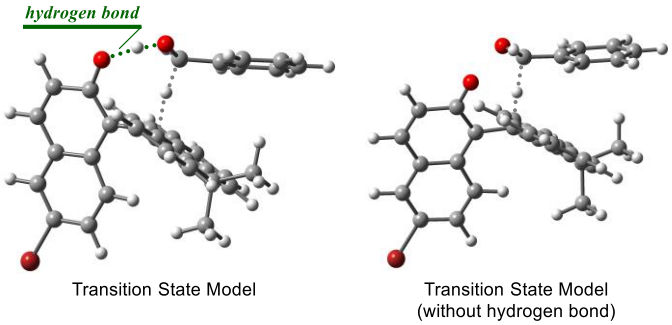

Figure 1 Transition state models for the dehydridation of primary benzylic alcohol with **2Br**.

Comparing the energy of this transition state structure (ΔG = 16.4 kcal/mol, SMD(CH_2Cl_2)-M06/cc-pVTZ level)[5,6] with that of the most stable transition state structure (ΔG = 24.1 kcal/mol) modeled for the stepwise dehydridation pathway without hydrogen-bonding interactions supported the importance of preorganization by hydrogen-bond for attaining sufficient reactivity. Next, we investigated the applicability of the oxidation protocol to other primary benzylic alcohols **5**. As seen in the representative results in Table 3, the electronic and steric nature of the *para*-substituent had only a minor effect on the reaction profile, and the corresponding methyl esters **7** were generally obtained in good yields (entries 3~9). This catalytic system was sensitive to the presence of *ortho*- or *meta*-substituents on the substrates, but it was capable for the oxidation of *meta*-chlorophenyl and *ortho*-methylphenyl methanols in moderate yields (entries 10 and 11).

Conclusion

The introduction of an overcrowded olefinic framework into the *o*-QM structure allowed it to function as surrogates for triarylmethylium ion. The design element was intended to induce structural distortion to enhance the contribution of the zwitterionic resonance form of *o*-QM, and its dehydridation activity was fully realized via photoexcitation. This feature of the newly devised *o*-QM enabled it to provide dehydridative catalytic activity for the oxidation of benzylic alcohols under aerobic photoirradiation conditions. The combination of experimental and computational investigations supports that the zwitterionic intermediate in the ground state acts as a dehydridation-active species and that *o*-QM is regenerated from its reduced form by either singlet oxygen or superoxide. We believe that this study provides valuable insights into the development of organic molecules capable of dehydridative catalysis and their synthetic applications.

General Information:

Infrared spectra were recorded on a SHIMADZU IRAffinity-1 spectrometer. UV-Vis absorption spectra were recorded on a Shimadzu UV-1800 spectrometer. ^{1}H NMR spectra were recorded on a JEOL JNM-ECZ400S (400 MHz), JEOL JNM-ECA500II (500 MHz), or JEOL JNM-ECA600II (600 MHz) spectrometer. Chemical shifts are reported in ppm from the solvent resonance (CD_3CN: 1.94 ppm, C_6D_6: 7.16 ppm) or tetramethylsilane (0.00 ppm; $CDCl_3$) resonance as the internal standard. Data are reported as follows: chemical shift, integration, multiplicity (s = singlet, d = doublet, t = triplet, m = multiplet, br = broad, brd = broad-doublet), and coupling constants (Hz). ^{13}C NMR spectra were recorded on a JEOL JNM-ECA600II (151 MHz) spectrometer with complete proton decoupling. Chemical shifts are reported in ppm from the solvent resonance ($CDCl_3$: 77.16 ppm, CD_3CN: 1.32 ppm, C_6D_6: 128.06 ppm). ^{19}F NMR spectra were recorded on a JEOL JNM-ECZ400S (376 MHz) spectrometer with complete proton decoupling. Chemical shifts are reported in ppm from benzotrifluoride (–64.0 ppm) resonance as the external standard. The high-resolution mass spectrometry were conducted on Thermo Fisher Scientific Exactive (ESI). Analytical thin layer chromatography (TLC) was performed on Merck precoated TLC plates (silica gel 60 F_{254}, 0.25 mm). Flash column chromatography was performed on Silica gel 60N (spherical neutral, 40-50 μm; Kanto Chemical Co., Inc.). Simple chemicals were purchased and used as such.

Experimental Section:

Detection of Hydrogen Peroxide:

Hydrogen peroxide (H_2O_2) was detected upon treatment with oxo[5,10,15,20-tetra-(4-pyridyl)porphyrinato]titanium (IV) (TiO(tpyp)) which is known to rapidly react with even trace amounts of H_2O_2. To a 50 μM solution of TiO(tpyp) in MeOH (2.0 mL) was added 0~0.8 mL of a 30% aqueous solution of H_2O_2. After being stirred for 5 min at room temperature, the mixture was analyzed by UV-Vis absorption spectroscopy measurement (A). A blank solution was prepared in a similar manner except for using distilled water instead of the sample solution and its absorbance was designated as A_B. The difference in absorbance was determined as follows: $\Delta A = A_B - A$. An increasing peak at 442 nm suggests the generation of the Ti(O_2)(tpyp) complex (Fig. S1).

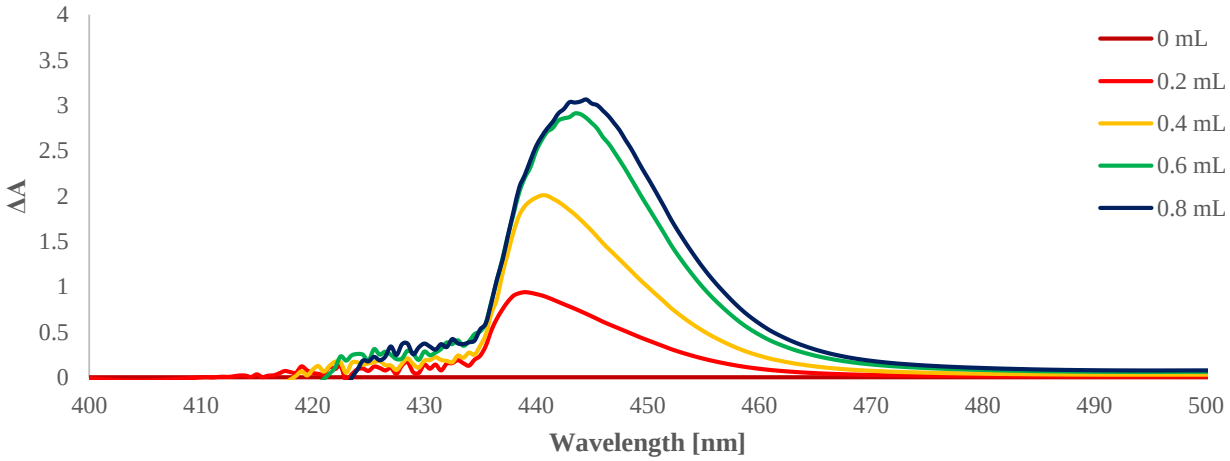

Figure S1. Difference in absorbance spectrum of TiO(tpyp) in MeOH with a varied amount of 30% H_2O_2 *aq*.

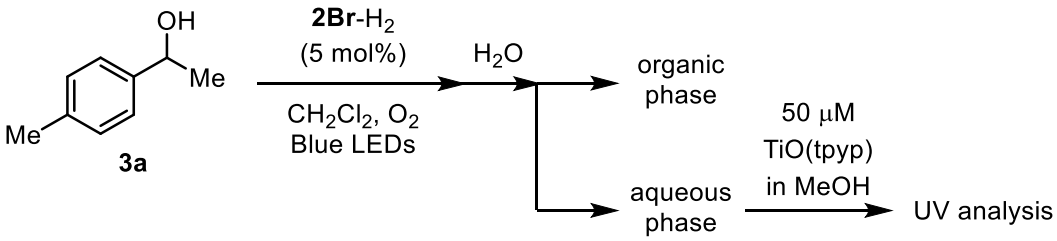

A solution of 1-(4-methylphenyl)ethyl alcohol (**3a**, 13.4 mg, 0.10 mmol) and **2Br**-H_2 (2.2 mg, 0.0050 mmol) in CH_2Cl_2 (4.0 mL) in a test tube was irradiated with Kessil PR160L-456 Blue LED lamps with fans under oxygen atmosphere for 12 h. Distilled water (2.0 mL) was added to the reaction mixture, and the aqueous and organic phases were separated. The aqueous phase (0~0.8 mL) was introduced to a 50 μM solution of TiO(tpyp) in MeOH (2.0 mL). After being stirred for 5 min at room temperature, the solution was analyzed by UV-Vis absorption spectroscopy measurement.

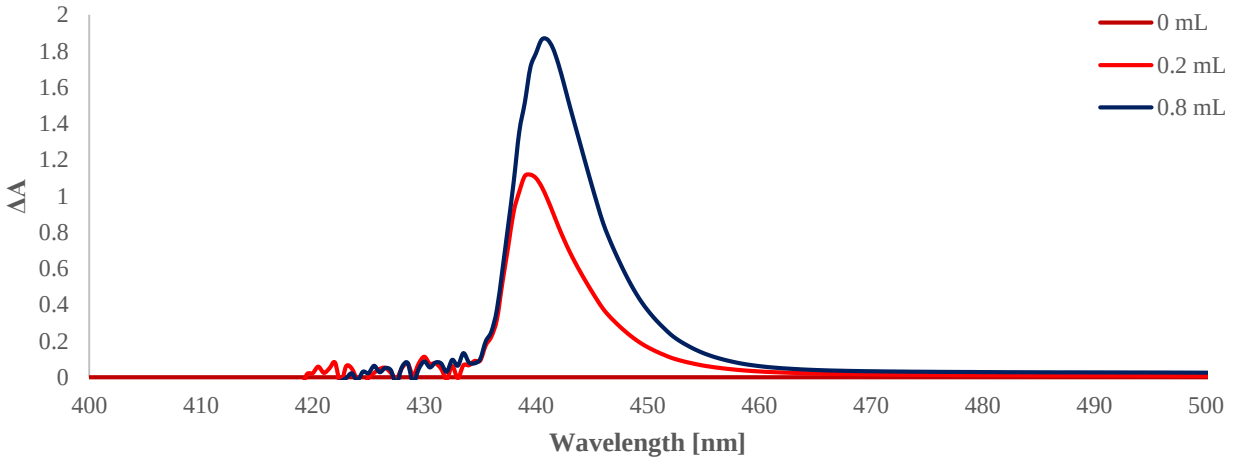

Figure S2. Difference in absorbance spectrum of TiO(tpyp) in MeOH with a different amount of an aqueous phase of the reaction mixture.

Representative Procedure for 2Br-H_2-catalyzed Oxidation of Secondary Benzylic Alcohols under Aerobic Photoirradiation Condition:

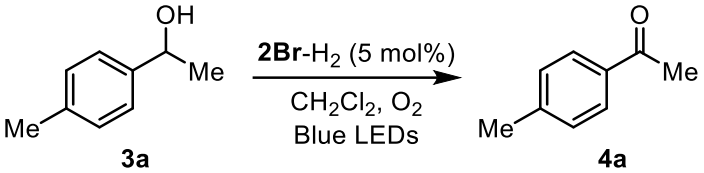

1-(4-Methylphenyl)ethyl alcohol (**3a**, 13.4 mg, 0.10 mmol), **2Br**-H_2 (2.2 mg, 0.0050 mmol), and CH_2Cl_2 (4.0 mL) were added to a test tube equipped with a stir bar. After bubbling with oxygen, the reaction mixture was irradiated with Kessil PR160L-456 Blue LED lamps (456 nm) with fans under oxygen atmosphere for 12 h. The reaction mixture was concentrated under reduced pressure. Purification of the residue was performed by column chromatography on Silica gel 60N (H/Et_2O = 10:1 as eluent) to afford 4'-methylacetophenone (**4a**) in 97% yield (13.2 mg, 0.097 mmol). **4a**[7]: ^{1}H NMR (400 MHz, $CDCl_3$) δ 7.86 (2H, d, J = 8.4 Hz), 7.25 (2H, d, J = 8.4 Hz), 2.57 (3H, s), 2.41 (3H, s).

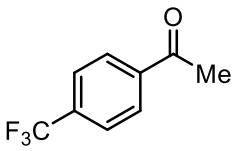

4'-(Trifluoromethyl)-acetophenone (4b)[8]**:** ^{1}H NMR (400 MHz, $CDCl_3$) δ 8.06 (2H, d, J = 8.0 Hz), 7.73 (2H, d, J = 8.0 Hz), 2.65 (3H, s).

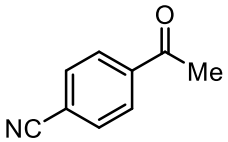

4'-Cyanoacetophenone (4c)[9]**:** ^{1}H NMR (400 MHz, $CDCl_3$) δ 8.05 (2H, td, J = 1.8, 8.6 Hz), 7.78 (2H, td, J = 1.8, 8.6 Hz), 2.65 (3H, s).

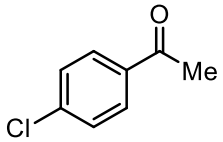

4'-Chloroacetophenone (4d)[7]: ^{1}H NMR (400 MHz, $CDCl_3$) δ 7.89 (2H, td, J = 2.3, 8.4 Hz), 7.44 (2H, td, J = 2.3, 8.4 Hz), 2.59 (3H, s).

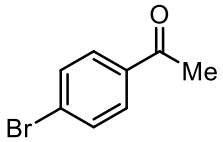

4'-Bromoacetophenone (4e)[7]: ^{1}H NMR (500 MHz, $CDCl_3$) δ 7.82 (2H, d, J = 8.5 Hz), 7.61 (2H, d, J = 8.5 Hz), 2.59 (3H, s).

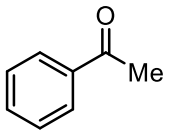

Acetophenone (4f)[9]: ^{1}H NMR (400 MHz, $CDCl_3$) δ 7.96 (2H, td, J = 1.6, 7.2 Hz), 7.57 (1H, tt, J = 1.6, 7.2 Hz), 7.47 (2H, tt, J = 1.6, 7.2 Hz), 2.61 (3H, s).

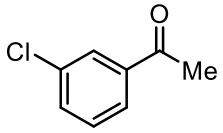

3'-Chloroacetophenone (4g)[7]: ^{1}H NMR (400 MHz, $CDCl_3$) δ 7.93 (1H, dd, J = 1.6, 2.0 Hz), 7.83 (1H, td, J = 1.6, 7.8 Hz), 7.54 (1H, ddd, J = 1.6, 2.0, 7.8 Hz), 7.41 (1H, t, J = 7.8 Hz), 2.60 (3H, s).

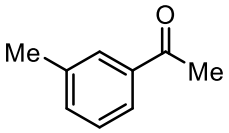

3'-Methylacetophenone (4h)[8]: ^{1}H NMR (400 MHz, $CDCl_3$) δ 7.78 (1H, s), 7.75 (1H, d, J = 7.6 Hz), 7.37 (1H, d, J = 7.6 Hz), 7.34 (1H, t, J = 7.6 Hz), 2.59 (3H, s), 2.41 (3H, s).

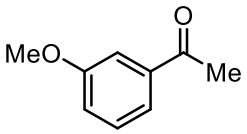

3'-Methoxyacetophenone (4i)[10]: ^{1}H NMR (400 MHz, $CDCl_3$) δ 7.54 (1H, td, J = 1.4, 8.2 Hz), 7.49 (1H, dd, J = 1.4, 2.6 Hz), 7.37 (1H, t, J = 8.2 Hz), 7.11 (1H, ddd, J = 1.4, 2.6, 8.2 Hz), 3.86 (3H, s), 2.59 (3H, s).

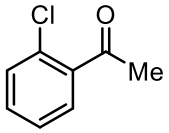

2'-Chloroacetophenone (4j)[7]: ^{1}H NMR (400 MHz, $CDCl_3$) δ 7.55 (1H, dd, J = 2.0, 8.0 Hz), 7.42 (1H, dd, J = 2.0, 8.0 Hz), 7.39 (1H, dt, J = 2.0, 8.0 Hz), 7.32 (1H, dt, J = 2.0, 8.0 Hz), 2.65 (3H, s).

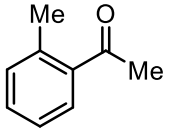

2'-Methylacetophenone (4k)[8]: ^{1}H NMR (400 MHz, $CDCl_3$) δ 7.68 (1H, d, J = 7.8 Hz), 7.37 (1H, t, J = 7.8 Hz), 7.26 (1H, t, J = 7.8 Hz), 7.24 (1H, d, J = 7.8 Hz), 2.58 (3H, s), 2.53 (3H, s).

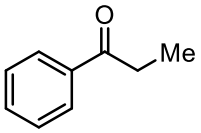

Propiophenone (4l)[9]: ^{1}H NMR (400 MHz, $CDCl_3$) δ 7.96 (2H, td, J = 1.6, 7.2 Hz), 7.55 (1H, tt, J = 1.6, 7.2 Hz), 7.45 (2H, tt, J = 1.6, 7.2 Hz), 3.00 (2H, q, J = 7.2 Hz), 1.23 (3H, t, J = 7.2 Hz).

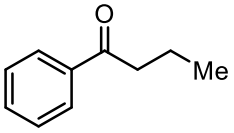

Butyrophenone (4m)[9]: ^{1}H NMR (500 MHz, $CDCl_3$) δ 7.96 (2H, d, J = 7.5 Hz), 7.56 (1H, t, J = 7.5 Hz), 7.46 (2H, t, J = 7.5 Hz), 2.95 (2H, t, J = 7.4 Hz), 1.77 (2H, sextet, J = 7.4 Hz), 1.01 (3H, t, J = 7.4 Hz).

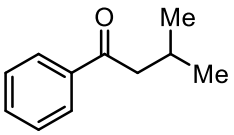

Isovalerophenone (4n)[11]: ^{1}H NMR (400 MHz, $CDCl_3$) δ 7.95 (2H, d, J = 7.5 Hz), 7.55 (1H, t, J = 7.5 Hz), 7.46 (2H, t, J = 7.5 Hz), 2.84 (2H, d, J = 6.6 Hz), 2.30 (1H, nonet, J = 6.6 Hz), 1.00 (6H, d, J = 6.6 Hz).

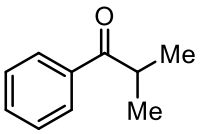

Isobutyrophenone (4o)[11]: ^{1}H NMR (400 MHz, $CDCl_3$) δ 7.56 (2H, d, J = 7.8 Hz), 7.55 (1H, t, J = 7.8 Hz), 7.46 (2H, t, J = 7.8 Hz), 3.56 (1H, septet, J = 6.8 Hz), 1.22 (6H, d, J = 6.8 Hz).

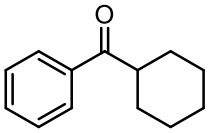

Cyclohexyl phenyl ketone (4p)[11]: ^{1}H NMR (500 MHz, $CDCl_3$) δ 7.94 (2H, d, J = 7.5 Hz), 7.54 (1H, t, J = 7.5 Hz), 7.46 (2H, t, J = 7.5 Hz), 3.26 (1H, tt, J = 3.3, 11.3 Hz), 1.89 (2H, brd, J = 13.0 Hz), 1.85 (2H, td, J = 3.3, 13.0 Hz), 1.78-1.71 (1H, m), 1.50 (2H, dq, J = 3.3, 13.0 Hz), 1.39 (2H, tq, J = 3.3, 13.0 Hz), 1.27 (1H, tq, J = 3.3, 13.0 Hz).

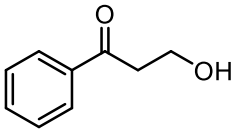

3-Hydroxypropiophenone (4q)[12]: ^{1}H NMR (600 MHz, $CDCl_3$) δ 7.97 (2H, d, J = 7.2 Hz), 7.95 (1H, t, J = 7.2 Hz), 7.48 (2H, t, J = 7.2 Hz), 4.04 (2H, t, J = 5.4 Hz), 3.24 (2H, t, J = 5.4 Hz), 2.76 (1H, br).

Procedure for Large Scale Oxidation of Benzylic Secondary Alcohol:

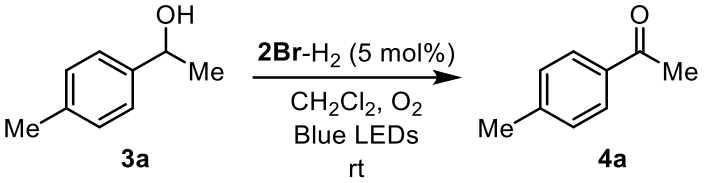

3a (681.0 mg, 5.0 mmol), **2Br**-H_2 (107.3 mg, 0.25 mmol), and CH_2Cl_2 (200 mL) were added to a 4-neck flask equipped with a condenser tube and stir bar. After bubbling with oxygen, the reaction mixture was irradiated with Kessil PR160L-456 Blue LED lamps (456 nm) with fans under oxygen atmosphere for 18 h. The reaction mixture was concentrated under reduced pressure. Purification of the residue was performed by column chromatography on Silica gel 60N (H/Et_2O = 10:1 as eluent) to afford **4a** in 74% yield (497.8 mg, 3.71 mmol).

Representative Procedure for 2Br-H_2O-catalyzed Oxidation of Primary Benzylic Alcohols under Aerobic Photoirradiation Condition:

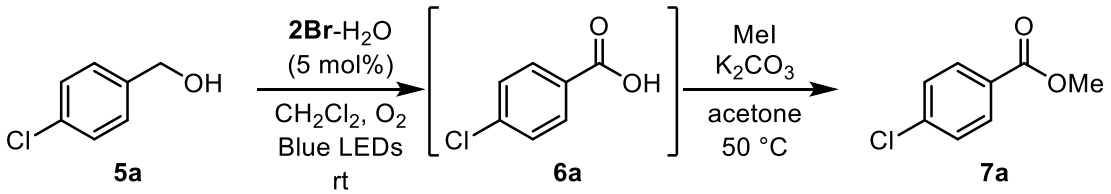

A solution of 4-chlorobenzyl alcohol (**5a**, 14.3 mg, 0.10 mmol) and **2Br**-H_2O (2.2 mg, 0.0050 mmol) in CH_2Cl_2 (4.0 mL) was saturated with oxygen by bubbling and irradiated with Kessil PR160L-456 Blue LED lamps (456 nm) with fans under oxygen atmosphere for 24 h. After concentration, the residue was treated with potassium carbonate (41.5 mg, 0.30 mmol) and iodomethane (141.9 mg, 1.0 mmol) in acetone (1.0 mL) at 50 °C for 5 h. Water was added to the reaction mixture and the aqueous phase was extracted with EA three times. The combined organic

extracts were washed with brine and dried over Na_2SO_4. After removal of volatiles under reduced pressure, purification of the crude mixture by column chromatography on silica gel 60N (H/Et_2O = 10:1 as eluent) afforded methyl 4-chlorobenzoate (**7a**) in 74% yield (12.6 mg, 0.074 mmol). **7a**[13]: ^{1}H NMR (400 MHz, $CDCl_3$) δ 7.97 (2H, td, J = 2.4, 8.4 Hz), 7.41 (2H, td, J = 2.4, 8.4 Hz), 3.91 (3H, s).

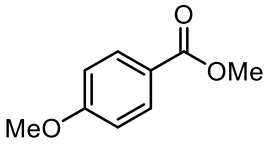

Methyl 4-methoxybenzoate (7b)[14]**:** ^{1}H NMR (400 MHz, $CDCl_3$) δ 7.99 (2H, td, J = 2.4, 9.2 Hz), 6.91 (2H, td, J = 2.4, 9.2 Hz), 3.88 (3H, s), 3.86 (3H, s).

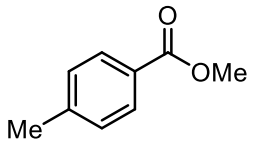

Methyl 4-methylbenzoate (7c)[14]**:** ^{1}H NMR (500 MHz, $CDCl_3$) δ 7.93 (2H, d, J = 8.0 Hz), 7.23 (2H, d, J = 8.0 Hz), 3.89 (3H, s), 2.40 (3H, s).

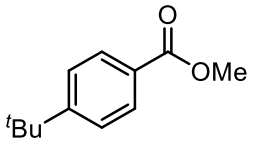

Methyl 4-*tert*-butylbenzoate (7d)[13]**:** ^{1}H NMR (400 MHz, $CDCl_3$) δ 7.96 (2H, td, J = 2.0, 8.8 Hz), 7.45 (2H, td, J = 2.0, 8.8 Hz), 3.90 (3H, s), 1.34 (9H, s).

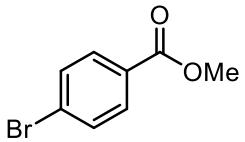

Methyl 4-bromobenzoate (7e)[13]**:** ^{1}H NMR (400 MHz, $CDCl_3$) δ 7.90 (2H, td, J = 2.1, 8.4 Hz), 7.58 (2H, td, J = 2.1, 8.4 Hz), 3.91 (3H, s).

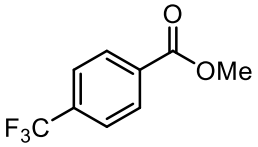

Methyl 4-(trifluoromethyl)-benzoate (7f)[14]**:** ^{1}H NMR (400 MHz, $CDCl_3$) δ 8.16 (2H. d, J = 8.0 Hz), 7.71 (2H, d, J = 8.0 Hz), 3.96 (3H, s).

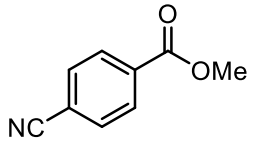

Methyl 4-cyanobenzoate (7g)[13]**:** ^{1}H NMR (400 MHz, $CDCl_3$) δ 8.14 (2H, td, J = 1.8, 8.4 Hz), 7.75 (2H, td, J = 1.8, 8.4 Hz), 3.96 (3H, s).

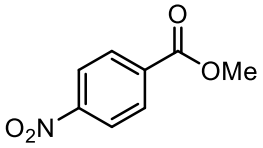

Methyl 4-nitrobenzoate (7h)[13]**:** ^{1}H NMR (400 MHz, $CDCl_3$) δ 8.29 (2H, td, J = 2.0, 8.4 Hz), 8.21 (2H, td, J = 2.0, 8.4 Hz), 3.98 (3H, s).

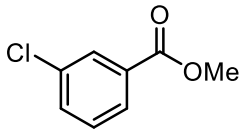

Methyl 3-chlorobenzoate (7i)[15]**:** ^{1}H NMR (400 MHz, $CDCl_3$) δ 8.02 (1H, t, J = 2.0 Hz), 7.92 (1H, td, J = 1.2, 8.0 Hz), 7.53 (1H, ddd, J = 1.2, 2.0, 8.0 Hz), 7.38 (1H, t, J = 8.0 Hz), 3.93 (3H, s).

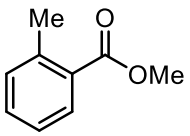

Methyl 2-methylbenzoate (7j)[16]**:** ^{1}H NMR (400 MHz, $CDCl_3$) δ 7.90 (1H, dd, J = 1.2, 7.6 Hz), 7.39 (1H, dt, J = 1.2, 7.6 Hz), 7.26-7.21 (2H, m), 3.89 (3H, s), 2.60 (3H, s).

Computational Details:

Transition States of Dehydridation Step of Oxidation of Primary Benzylic Alcohol: Geometry optimization was performed at the M06/cc-PVTZ level of theory. The CH_2Cl_2 solvent effects were taken into account by using the SMD model.

Cartesian Coordinates of Calculated Structures

2Br ($^1S_0$) E = -3651.06448467 a.u.

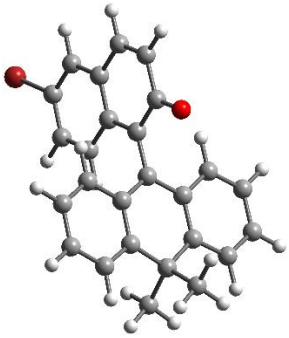

C	0.009036	-0.000300	1.302878
C	0.092316	-0.000786	2.755768
C	-1.154946	-0.000992	3.515974
C	-2.348170	-0.000839	2.891503
C	-2.452234	-0.000395	1.447741
C	-3.698847	-0.000279	0.815698
C	-3.792736	0.000170	-0.569528
C	-2.632740	0.000510	-1.351889
C	-1.388103	0.000386	-0.748554
C	-1.267468	-0.000083	0.659552
O	1.199876	-0.000825	3.331716
H	-1.072165	-0.001310	4.598438
H	-3.272561	-0.001040	3.463589
H	-4.599008	-0.000534	1.424275
H	-2.708547	0.000865	-2.434904
H	-0.490903	0.000628	-1.357842
C	1.257858	-0.000111	0.539513
C	1.864165	-1.250624	0.164410
C	1.277806	-2.473360	0.560967
C	1.839047	-3.690573	0.213388
C	3.005505	-3.713955	-0.546504
C	3.592914	-2.514904	-0.943726
C	3.051908	-1.275512	-0.604244
C	3.753721	0.000258	-1.073428
C	3.052009	1.275813	-0.603510
C	3.592912	2.515363	-0.942579
C	3.005462	3.714228	-0.544861
C	1.839042	3.690495	0.215080
C	1.277824	2.473122	0.562131
C	1.864202	1.250569	0.165032
C	3.800205	0.000778	-2.619186
C	5.199517	-0.000035	-0.524746
H	0.369012	-2.458418	1.153257
H	1.369759	-4.616109	0.534217
H	3.460443	-4.658340	-0.830453
H	4.501807	-2.558430	-1.535148
H	4.501733	2.559159	-1.534092
H	3.460340	4.658749	-0.828457
H	1.369724	4.615885	0.536285
H	0.369015	2.457903	1.154391
H	4.326034	0.884142	-2.993266
H	2.789927	0.000803	-3.041784
H	4.326259	-0.882181	-2.993887
H	5.201711	-0.000339	0.570068
H	5.747057	0.882347	-0.867049
H	5.746843	-0.882369	-0.867529
Br	-5.509621	0.000329	-1.406432

2Br-H$_2$ (S_0) E = -3652.32637635 a.u.

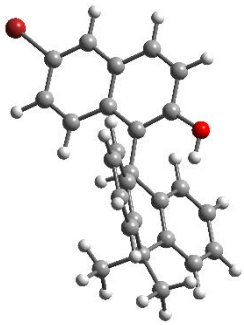

C	3.349164	0.000424	-2.692593
H	3.728019	0.888547	-3.209900
H	2.258910	0.000459	-2.780275
H	3.727998	-0.887586	-3.210107
C	-1.804224	-0.000017	-1.012699

H	-1.042580	0.000021	-1.783040
C	1.093147	-0.000033	-0.145012
H	0.684525	0.000052	-1.157722
C	-0.082477	-0.000209	0.821681
C	4.016937	-2.433000	-0.446048
H	5.041295	-2.453928	-0.797171
C	1.947723	1.265846	-0.053363
C	3.267077	-1.254480	-0.535718
C	3.480169	-3.602186	0.083046
H	4.090971	-4.498991	0.138609
C	1.411136	2.448799	0.462313
H	0.387485	2.458200	0.822053
C	3.479700	3.602390	0.083860
H	4.090382	4.499265	0.139620
C	1.411452	-2.448953	0.461764
H	0.387801	-2.458561	0.821502
C	1.947884	-1.265818	-0.053653
C	5.360399	0.000315	-1.240732
H	5.790445	0.000354	-0.233539
H	5.739907	0.872509	-1.777380
H	5.739955	-0.871892	-1.777331
C	2.164355	3.614611	0.532134
H	1.725785	4.520580	0.940715
C	3.266922	1.254789	-0.535427
C	3.825801	0.000264	-1.216959
O	1.383241	-0.000507	2.748075
H	2.084758	-0.000371	2.076411
C	4.016624	2.433393	-0.445491
H	5.040979	2.454537	-0.796601
C	2.164827	-3.614681	0.531324
H	1.726381	-4.520800	0.939707
C	0.143250	-0.000403	2.186118
C	-1.441693	-0.000151	0.364529
C	-0.914461	-0.000505	3.125342
H	-0.663127	-0.000655	4.181585
C	-2.508857	-0.000227	1.312284
C	-3.113734	0.000056	-1.420432
H	-3.352885	0.000151	-2.478586
C	-3.857525	-0.000138	0.876306
H	-4.647591	-0.000190	1.620849
C	-2.209468	-0.000406	2.698894
H	-3.026328	-0.000472	3.415188
C	-4.142975	0.000006	-0.459372
Br	-5.948741	0.000135	-1.050621

BnOH *E* = -346.648953098 a.u.

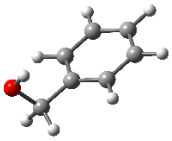

C	-0.183368	-1.170785	-0.199977
C	-1.551404	-1.244452	0.041960
C	-2.297458	-0.075849	0.198451
C	-1.668123	1.162818	0.111144
C	-0.296525	1.231648	-0.130665
C	0.459251	0.068389	-0.285533
H	0.395849	-2.082815	-0.323522
H	-2.039176	-2.213369	0.104117
H	-3.366235	-0.132907	0.385181
H	-2.243544	2.076942	0.228618
H	0.192389	2.200548	-0.202696
C	1.948419	0.143682	-0.512385
H	2.225133	1.145324	-0.864024
O	2.704501	-0.192626	0.655361
H	2.473289	0.434137	1.360777
H	2.261536	-0.579556	-1.269311

TS$_{concerted}$ *E* = -3997.71405992 a.u.

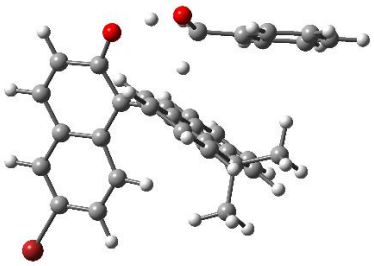

C	-0.618227	1.429102	-0.347328
C	-0.496879	2.771887	-0.783727
C	-1.685673	3.430668	-1.279832

C	-2.904828	2.842783	-1.278643
C	-3.076343	1.537612	-0.729295
C	-4.366587	0.969861	-0.649178
C	-4.543900	-0.252934	-0.057452
C	-3.454429	-0.936063	0.503034
C	-2.193011	-0.395108	0.416700
C	-1.936258	0.840292	-0.238921
O	0.591152	3.465123	-0.812832
H	-1.545138	4.437072	-1.663520
H	-3.774802	3.365409	-1.669033
H	-5.206592	1.526044	-1.054021
H	-3.603190	-1.880823	1.015351
H	-1.385586	-0.938907	0.887839
C	0.557314	0.583765	0.067112
C	0.620837	-0.783401	-0.506608
C	0.141504	-0.979730	-1.814894
C	0.173901	-2.224878	-2.411462
C	0.700479	-3.304426	-1.700310
C	1.195575	-3.114730	-0.419460
C	1.180512	-1.857407	0.200046
C	1.700949	-1.730323	1.626082
C	1.691585	-0.291616	2.132723
C	2.190275	-0.031733	3.415161
C	2.160249	1.238972	3.970113
C	1.601281	2.298096	3.255963
C	1.085507	2.063572	1.995691
C	1.128971	0.781111	1.414446
C	3.136551	-2.296223	1.703554
C	0.785384	-2.572865	2.549653
H	-0.266006	-0.132262	-2.356264
H	-0.206607	-2.358712	-3.419587
H	0.727726	-4.294190	-2.147133
H	1.597905	-3.969969	0.112516
H	2.605596	-0.843196	4.002587
H	2.562504	1.400393	4.966267
H	1.564449	3.295642	3.682882
H	0.644369	2.879857	1.438112
H	3.515048	-2.258654	2.728121
H	3.819662	-1.729551	1.065511
H	3.161146	-3.342070	1.387934
H	-0.246295	-2.207769	2.522667
H	1.136216	-2.529499	3.584533
H	0.785733	-3.621349	2.237929
H	1.645407	1.091699	-0.703317
C	2.640068	1.618813	-1.294458
H	2.112139	1.818203	-2.235283
O	2.940281	2.704711	-0.565055
H	2.045176	3.200709	-0.551997
C	3.701437	0.596710	-1.393832
C	3.645202	-0.358129	-2.415692
C	4.781543	0.591625	-0.503295
C	4.654815	-1.304725	-2.546979
H	2.814960	-0.346667	-3.115606
C	5.796078	-0.347905	-0.645164
H	4.827290	1.336537	0.284048
C	5.733292	-1.298268	-1.664083
H	4.605883	-2.040285	-3.344512
H	6.638122	-0.340952	0.040888
H	6.527152	-2.031987	-1.771992
Br	-6.277622	-1.026567	0.048005

TS$_{stepwise}$ E = -3997.70356472 a.u.

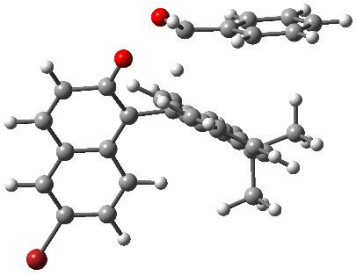

C	-0.602455	1.442185	0.043020
C	-0.464581	2.866617	-0.085605
C	-1.668024	3.616361	-0.377634
C	-2.886073	3.048779	-0.439658
C	-3.054089	1.655443	-0.214149
C	-4.341371	1.100577	-0.208368
C	-4.518602	-0.230326	0.047838
C	-3.422011	-1.044454	0.330067
C	-2.159566	-0.512272	0.320139

C	-1.907619	0.848501	0.026420
O	0.626988	3.475221	-0.005925
H	-1.531610	4.680997	-0.528048
H	-3.769243	3.645452	-0.642917
H	-5.187780	1.748998	-0.403048
H	-3.565723	-2.090842	0.565881
H	-1.340752	-1.170330	0.570241
C	0.608980	0.595178	0.155631
C	1.331423	0.509013	1.447617
C	1.488841	1.664006	2.225896
C	2.150116	1.632639	3.429890
C	2.651021	0.427070	3.899944
C	2.485326	-0.717777	3.152594
C	1.848115	-0.707845	1.910209
C	1.658817	-2.026523	1.184961
C	1.146679	-1.836621	-0.225519
C	1.108313	-2.932526	-1.088007
C	0.615661	-2.831953	-2.371780
C	0.138847	-1.614072	-2.836484
C	0.147475	-0.527704	-1.993489
C	0.636693	-0.621640	-0.683345
C	0.626463	-2.852792	1.976363
C	2.970185	-2.819011	1.134571
H	1.108545	2.598236	1.835740
H	2.271374	2.540870	4.005714
H	3.161950	0.378580	4.853119
H	2.859184	-1.650937	3.552773
H	1.466608	-3.893921	-0.743278
H	0.600987	-3.704620	-3.011845
H	-0.250096	-1.521644	-3.841883
H	-0.253961	0.419754	-2.330039
H	0.340902	-3.746749	1.418800
H	-0.275216	-2.274686	2.186710
H	1.048584	-3.172013	2.931323
H	3.653811	-2.401518	0.394165
H	2.782174	-3.860920	0.873793
H	3.476721	-2.822740	2.097515
H	1.512837	1.347873	-0.533139
C	2.428774	1.836597	-1.369210
C	3.543385	0.893625	-1.270188
C	4.365174	0.978164	-0.144236
C	3.840053	-0.043553	-2.257676
C	5.483580	0.176973	-0.031020
H	4.134914	1.706493	0.624738
C	4.965249	-0.838812	-2.144659
H	3.198388	-0.171335	-3.122952
C	5.794863	-0.721142	-1.040440
H	6.114978	0.256497	0.844063
H	5.199508	-1.550131	-2.925532
H	6.682851	-1.334879	-0.963867
H	2.558728	2.764962	-0.822409
O	1.785433	2.025548	-2.529446
H	1.871956	1.253625	-3.106042
Br	-6.263653	-0.984499	0.042321

References

(1) (a) Matsubara, C.; Kawamoto, N.; Takamura, K. *Analyst* **1992**, *117*, 1781–1784. (b) Uraguchi, D.; Torii, M.; Ooi, T. *ACS Catal.* **2017**, *7*, 2765–2769.

(2) (a) Draper, W. M.; Crosby, D. G. *J. Agric. Food Chem.* **1983**, *31*, 734–737. (b) Hayyan, M.; Ali Hashim, M.; AlNashef, I. M. *Chem. Rev.* **2016**, *116*, 3029–3085.

(3) (a) Wang, J.; Liu, C.; Yuan, J.; Lei, A. *New J. Chem.* **2013**, *37*, 1700–1703. (b) Nikitas, N. F.; Tzaras, D. I.; Triandafillidi, I.; Kokotos, C. G. *Green Chem.* **2020**, *22*, 471–477.

(4) (a) Wan, P.; Chak, B. *J. Chem. Soc., Perkin Trans. 2* **1986**, 1751–1756. (b) Toteva, M. M.; Richard, J. P. *Adv. Phys. Org. Chem.* **2011**, *45*, 39–91.

(5) Zhao, Y.; Truhlar, D. Theor. *Chem. Acc.* **2008**, *120*, 215−241.

(6) Dunning Jr., T. H. *J. Chem. Phys.* **1989**, *90*, 1007−1023.

(7) Budweg, S.; Wei, Z.; Jiao, H.; Junge, K.; Beller, M. *ChemSusChem* **2019**, *12*, 2988−2993.

(8) Wang, Q.; Chai, H.; Yu, Z. *Organometallics* **2018**, *37*, 584−591.

(9) Kim, M. J.; Jung, Y. E.; Lee, C. Y.; Kim, J. *Tetrahedron Lett.* **2018**, *59*, 2722−2725.

(10) Muthaiah, S.; Hong, S. H. *Adv. Synth. Catal.* **2012**, *354*, 3045−3053.

(11) Lei, C.; Zhu, D.; Tangcueco III, V. T.; Zhou, J. S. *Org. Lett.* **2019**, *21*, 5817−5822.

(12) Kirihara, M.; Kakuda, H.; Ichinose, M.; Ochiai, Y.; Takizawa, S.; Mokuya, A.; Okubo, K.; Hatano, A.; Shiro, M. *Tetrahedron* **2005**, *61*, 4831−4839.

(13) Hirashima, S.-i.; Nobuta, T.; Tada, N.; Miura, T.; Itoh, A. *Org. Lett.* **2010**, *12*, 3645–3647.

(14) Liu, C.; Wang, J.; Meng, L.; Deng, Y.; Li, Y.; Lei, A. *Angew. Chem. Int. Ed.* **2011**, *50*, 5144–5148.

(15) Molander, G. A.; Cavalcanti, L. N. *J. Org. Chem.* **2011**, *76*, 7195–7203.

(16) Heller, S. T.; Sarpong, R. *Org. Lett.* **2010**, *12*, 4572–4575.